

Table 1. IDO Inhibition from Commercially Available Quinone Structures

	compd	IC ₅₀ (μM)	E (mV)		compd	IC ₅₀ (μM)	E (mV)
1	2,3-dichloro-1,4-naphthoquinone	0.28	−604 ²²	7	2-hydroxy-1,4-naphthoquinone	~675	−357 ²³
2	2-methoxy-1,4-naphthoquinone	0.72		8	benzoquinone	no activity	−401 ²⁴
3	1,4-naphtho-quinone	0.99	−140 ²⁵	9	2-methyl-1,4-benzoquinone	no activity	−466 ²⁴
4	5-hydroxy-1,4-naphthoquinone	1.0	−93 ²⁶	10	2-phenyl-1,4-benzoquinone	no activity	
5	2-methyl-1,4-naphthoquinone	1.1	−203 ²⁷	11	vitamin K1	no activity	−170 ²⁸
6	1,2-naphthoquinone	7.1	−89 ²⁵	12	chromone	no activity	

IC₅₀ (inhibitory concentration 50%) is the concentration of compound that inhibits enzyme activity by half. E is the reduction potential for the one electron reduction of the quinone to the semiquinone.

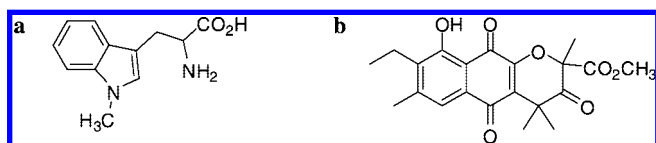


Figure 1. Structure of two small molecule inhibitors of IDO: (a) 1-methyl-tryptophan (IMT), a widely used IDO inhibitor that is bioactive; (b) annulin B, a potent IDO inhibitor isolated from a marine invertebrate, which lacks an indole core structure.

Herein, we describe the discovery of highly potent IDO inhibitors that lack the indole core of IDO's natural substrate. These potent inhibitors are inspired by the natural product annulin B^{20,21} (Figure 1) and contain naphthoquinone as the key pharmacophore. In this study, we demonstrate through mouse tumor models that the naphthoquinone natural product, menadione, has antitumor activity mediated through IDO inhibition. Furthermore, we describe the synthesis and characterization of a new structural class of IDO inhibitors based on the naphthoquinone pharmacophore. The most active compounds are pyranonaphthoquinones, and they represent the most potent IDO inhibitors described to date.

Results

Naphthoquinone Is the Pharmacophore of Natural Product Annulin B. Andersen et al. recently described^{20,21} several natural products isolated from a marine hydroid with potent activity as IDO inhibitors, the most potent of which was annulin B with a $K_i = 0.12 \mu\text{M}$. Most of the marine natural product inhibitors contained a naphthoquinone core, and by comparing the structure of IMT with annulin B (Figure 1), we hypothesized that the relevant pharmacophore in annulin B was the naphthoquinone core. In support of the notion that naphthoquinone is an indole mimetic, commercially available compounds containing a quinone structure were screened for IDO inhibitory activity and several demonstrated micromolar levels of inhibitory potency (Table 1). The 1,2- or 1,4-naphthoquinone unit was essential for activity (cf. **1–6** vs **8–10**, **12**), and substitution was permitted on either the benzene (e.g., **4**) or the quinone ring (e.g., **1**, **2**, and **5**) of the naphthoquinone core. Exceptions to this principle were found with the phytylated 1,4-naphthoquinone derivative vitamin K1 and the 2-hydroxy derivative **7**; the latter was particularly noteworthy given the activity of the structurally analogous 1,2-naphthoquinone **6**. All benzoquinone derivatives were inactive, thereby confirming the need for a fused benzene-quinone structure for activity as an IDO inhibitor. Although quinones are well-known oxidants, there was no apparent correlation between the IDO inhibitory potency and the reduction potential of these different quinone-based compounds (Table 1).

IDO Is an Essential Target for the Antitumor Activity of the Naphthoquinone Menadione. Included among the naphthoquinone-based compounds evaluated for IDO inhibitory activity was menadione, also known as vitamin K3 (**5**), which exhibited low micromolar potency (IC₅₀ = 1.0 μM) (Table 1).

Table 2. IC₅₀ Values for Glutathione-Conjugated Menadione (Quinone and Hydroquinone Forms)

	compound	IC ₅₀ (μM)
13		0.88
14		0.34

This was a specific feature of this vitamin K precursor molecule, as vitamin K1 (**11**) lacked activity as an IDO inhibitor. Although other naphthoquinones in our initial screen were more potent, menadione is a known anticancer agent²⁹ and clinical studies have provided evidence of its activity as a radiosensitizer and its ability to cooperate with chemotherapeutic agents, reminiscent of other IDO inhibitors.^{4,14} Consequently, we chose to explore the *in vivo* activity of the naphthoquinones with menadione.

While a variety of hypotheses for the mechanism of action of menadione have been proposed, a definitive understanding has yet to emerge. Most studies have focused on its ability to generate reactive oxygen species (ROS) or to deplete intracellular glutathione through the formation of menadione–glutathione and glutathione–glutathione conjugates,³⁰ which may have cytotoxic consequences.³¹ Interestingly, we found that the glutathione conjugate of menadione (both in quinone **13** and hydroquinone **14** forms) retained IDO inhibitory activity, exhibiting even greater potencies than the parent compound (Table 2). In a cell-based assay, the IC₅₀ of menadione for IDO inhibition was determined to be lower than the LD₅₀ for cellular cytotoxicity by >4-fold (Figure 2a), indicating that there is a window between IDO inhibitory activity and general cytotoxicity for this compound.

Based on available information in the NCI database about menadione in different mouse models of cancer (<http://dtp.nci.nih.gov/dtpstandard/InvivoSummary/index.jsp>), we evaluated whether menadione, administered at levels near the maximum tolerated dose (MTD), would cooperate with paclitaxel in the MMTV-*Neu* transgenic mouse model of breast cancer, an assay where the antitumor efficacy of various IDO inhibitors has previously been demonstrated.^{14,32} Administration of menadione alone at 25 mg/kg once a day (qd) resulted in some evidence of growth inhibition, while the same dose administered twice a day (bid) was lethal, indicating that no further dose escalation would be possible. However, like other IDO inhibitors, which

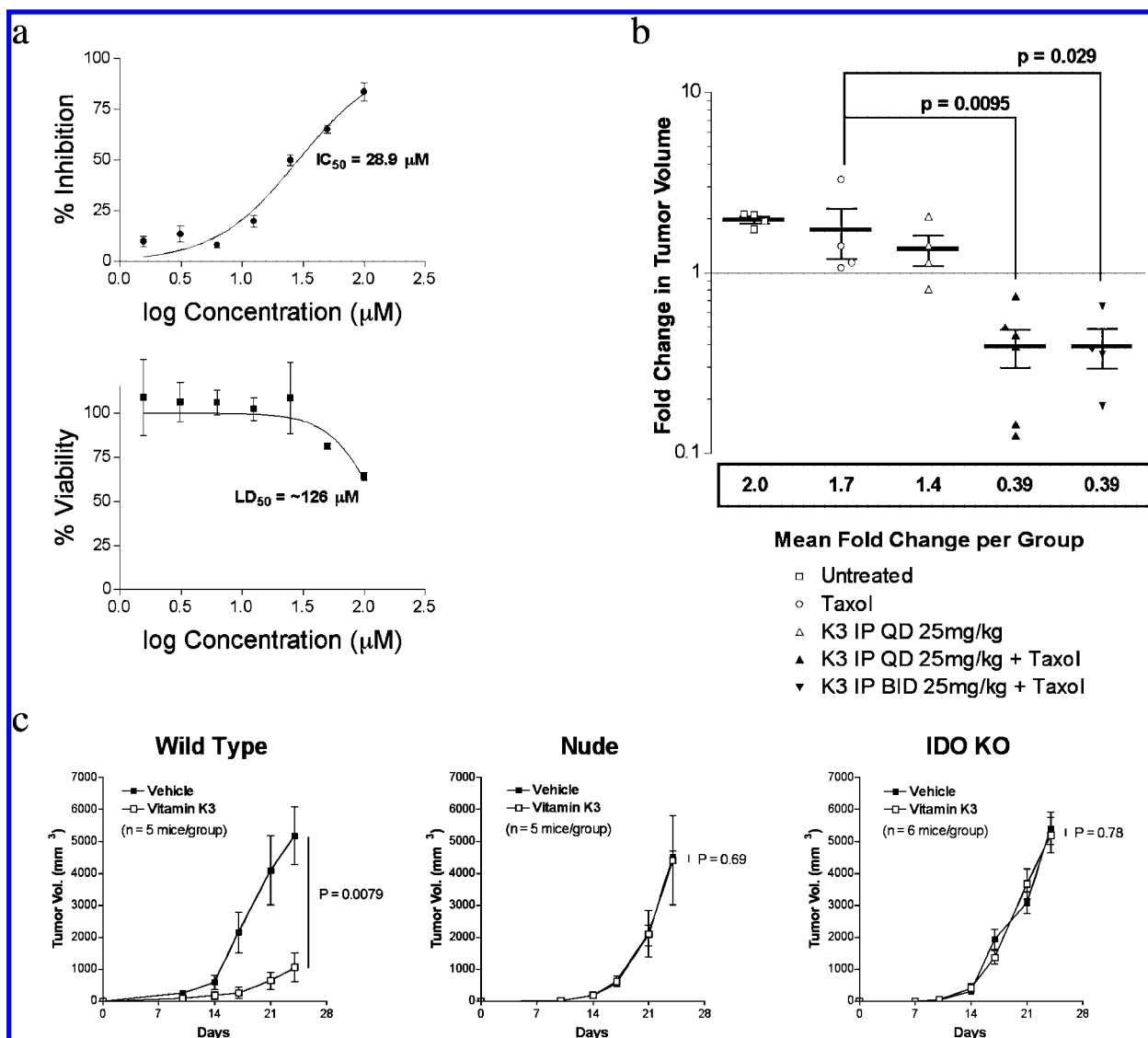


Figure 2. *In vivo* validation of IDO as an essential target of menadione antitumor activity. (a) Cell-based comparison of IDO inhibition and cytotoxicity of menadione. A clonal T-REx-derived cell line, stably transfected with doxycyclin-inducible IDO, was exposed to a range of menadione concentrations. The top graph shows the percent inhibition of IDO activity (adjusted for cell viability) based on comparison of kynurenine levels in the culture supernatant of menadione-exposed cells to that of untreated controls. The bottom graph shows the percent viability of the same cells used for the IDO inhibition assay based on SRB assay results from menadione-exposed cells compared to untreated controls. IC_{50} and LD_{50} values were determined from the sigmoidal dose-response curves. The assays were performed in triplicate and graphed as means \pm SD. (b) Menadione effectively combines with paclitaxel chemotherapy to regress established breast tumors. Parous MMTV-*Neu* mice with 0.5–1.0 cm mammary gland tumors were randomly enrolled for 2-week treatment studies. Tumor volume determinations were made at the beginning and end of the treatment period. Cohorts receiving menadione (K3) were administered compound i.p. either once a day (qd) or twice a day (bid) as indicated at 25 mg/kg for 5 consecutive days during the first week of treatment. Paclitaxel (Taxol) was administered to the indicated cohorts i.v. at 13.3 mg/kg qd 3 \times /week over the entire course of the 2-week treatment period. Each point represents the fold change in volume for an individual tumor with the mean \pm SEM indicated for each group. The significance of the differences between the paclitaxel alone and the paclitaxel + menadione treatment groups was assessed using a nonparametric two-tailed Mann-Whitney test to determine the indicated P values. (c) Menadione suppresses outgrowth of B16-F10 tumors in a T cell and host IDO dependent manner. Menadione treatment, administered i.p. at 25 mg/kg qd 5 days a week until termination of the experiment, was initiated 7 days following s.c. injection of C57BL/6 mice with 1×10^5 B16-F10 melanoma-derived cells. Caliper measurements of tumors were performed biweekly until the control tumors reached a volume of $\sim 5000 \text{ mm}^3$. From left to right are the results obtained from C57BL/6 mice, athymic NCr-nu/nu mice, and C57BL/6-strain, IDO knockout mice as indicated above each graph, plotted as mean tumor size \pm SEM at each time point. At the conclusion of each study, the difference in tumor volumes between the treatment and nontreatment groups was assessed using a nonparametric two-tailed Mann-Whitney test to determine the P value indicated on each graph.

also display weak antitumor activity on their own,¹⁴ combining menadione at the 25 mg/kg qd dose with paclitaxel produced significant tumor regressions in the model (Figure 2b). Surprisingly, mice receiving the combination of paclitaxel with menadione at 25 mg/kg bid all survived; however, the antitumor response was similar irrespective of whether the compound was administered once or twice daily (Figure 2b).

To validate the requirement of IDO as a target for the antitumor efficacy of menadione, we compared the activity of this compound in a mouse model of cancer where we could genetically assess the consequences of IDO loss. Briefly, tumors formed by the mouse melanoma cell line B16-F10 do not express IDO *in vitro* or *in vivo*.³³ Nevertheless, growth of tumor isografts formed by these cells can be suppressed significantly

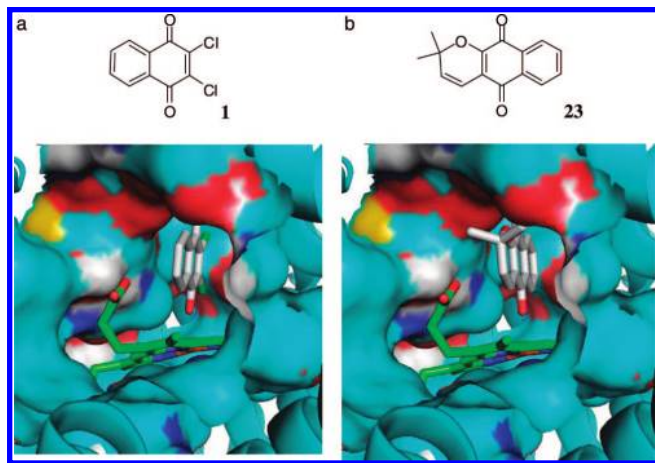


Figure 3. Docking naphthoquinones at the IDO active site by molecular modeling. (a) Proposed binding mode of compound **1** in IDO active site. (b) Proposed binding mode of pyranonaphthoquinone **23** in IDO active site. Graphics generated with PyMOL 098 (<http://www.py-mol.org>), an open-source molecular graphics system developed supported and maintained by DeLano Scientific LLC (<http://www.delano-scientific.com>).

by single agent treatment with an IDO inhibitor,³² due, presumably, to inhibition of IDO expressed in tolerogenic dendritic cells that accumulate in tumor draining lymph nodes of the host animal.³³ In this model, we confirmed that the growth of B16-F10 isograft tumors could be reduced significantly by single agent menadione treatment (Figure 2c). In contrast, we detected no growth inhibition of tumor grafts in either athymic nude mice or syngeneic IDO knockout mice (Figure 2c). These findings indicate that the antitumor activity of menadione requires both IDO inhibition and T cell involvement, thereby validating IDO as a critical therapeutic target for menadione—a prototypical representative of the naphthoquinone class of IDO inhibitors.

Molecular Modeling with Naphthoquinone Leads. We noted that the commercially available naphthoquinone structures with activity as IDO inhibitors generally displayed a noncompetitive mode of inhibition (Table 1). Noncompetitive or uncompetitive modes of inhibition usually suggest a basis in allosteric binding; however, there exists a precedent for IDO inhibitors to bind at the active site and yet display noncompetitive or uncompetitive kinetics. For example, 4-phenylimidazole (4-PI) has been reported to bind preferentially to the heme iron in the inactive ferric form of IDO.^{34,35} Also, β -carboline has been reported to compete with oxygen for ferrous heme iron binding.³⁴ Nonetheless, in a mechanistic study, both 4-PI and β -carboline demonstrated noncompetitive kinetics,³⁴ while the original report describing β -carboline as an IDO inhibitor reported uncompetitive inhibition.³⁶ Consequently, noncompetitive inhibition of IDO may not preclude heme iron binding at the active site by the naphthoquinone derivatives. Monodentate heme iron binding by quinones is not common,³⁷ but several recent studies of photosynthesis and, particularly one involving study of cytochrome *b₆f*,^{38,39} have demonstrated monodentate iron heme binding by quinones.

Utilizing the recently reported crystal structure of IDO,³⁵ computational docking studies in the absence of molecular oxygen placed several naphthoquinones at the active site with the quinone oxygen coordinated to the heme iron. Furthermore, the docking studies showed that the orientation of a particular naphthoquinone will depend on the substituents on the naphthoquinone core. With relatively small substituents on the C-2 or C-3 position (e.g., **1**), the naphthoquinone entered the active

Scheme 1. General Synthetic Path to Pyranonaphthoquinone Derivatives

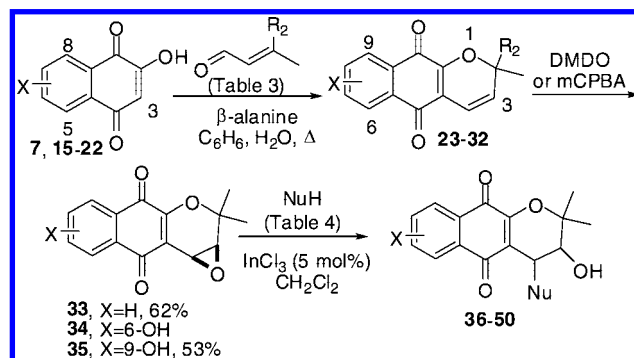


Table 3. 6 π Electrocyclization Reactions

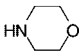
naphthoquinone		product			
	X		X	R ₂	yield(%)
7	H	23	H	CH ₃	77
7	H	24	H	CO ₂ CH ₃	22
15	5-OH	25	6-OH	CH ₃	69
16	5-OCH ₃	26	6-OCH ₃	CH ₃	76
17	6-OH	27	7-OH	CH ₃	71
18	6-OCH ₃	28	7-OCH ₃	CH ₃	71
19	7-OH	29	8-OH	CH ₃	75
20	7-OCH ₃	30	8-OCH ₃	CH ₃	72
21	8-OH	31	9-OH	CH ₃	56
22	8-OCH ₃	32	9-OCH ₃	CH ₃	52

site with the benzene ring projecting toward the entrance of the active site (Figure 3a). In contrast, tricyclic pyranonaphthoquinones, such as **23**, which include the pyran ring of annulin B, entered with the benzene ring projecting into the posterior of the active site (Figure 3b). Similarly, docking of annulin B confirmed that the substituted benzene ring is nestled in the back of the IDO active site, with the pyran ring located at the opening of the active site (data not shown). These docking studies provided an initial working model to direct synthetic modifications to the naphthoquinone core to improve potency.

Synthesis of Novel Pyranonaphthoquinone Inhibitors of IDO. Initial efforts were directed at mimicking the structure of annulin B, by installing and elaborating the pyran ring through chemical syntheses. Naphthoquinones **7** and **15–22** were easily converted to pyranonaphthoquinones **23–32** via a one-pot 6 π electrocycloization reaction in modest to good yield (Scheme 1 and Table 3).^{40–42} The naphthoquinones with substituents in the benzene ring were synthesized according to literature procedures. Epoxidation of **23** proceeded with dimethyldioxirane to afford **33**, while epoxidation of **25** and **31** was accomplished with *m*-CPBA to provide **34** and **35**, respectively. Further derivatization of the pyran ring was accomplished by nucleophilic substitution of the epoxides (Scheme 1 and Table 4). The cis and trans diastereomers (**36–50**) were separable by column chromatography. Assignment of the cis and trans diastereomers was based on an X-ray crystal structure of **36** (Supporting Information) and an analysis of NMR coupling constants. Hydrogenation, bromohydrin formation, and dihydroxylation⁴¹ were also employed to selectively modify the pyran alkene (Scheme 2).

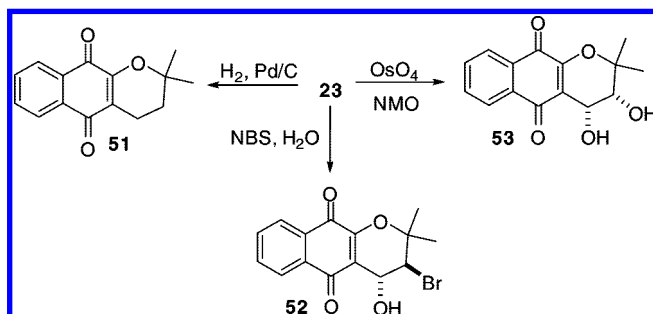
Evaluation of Pyran Ring Derivatives. The docked binding mode of annulin B, with its pyran ring located at the opening of the active site, suggested focusing synthesis on the pyran ring as a means of embellishing the naphthoquinone core and restoring or enhancing the level of IDO inhibition displayed

Table 4. Epoxide Opening Reactions

epoxide	NuH	cis (yield, %)	trans (yield, %)
33 (X=H)	PhCH ₂ NH ₂	36 (53)	37 (37)
33	CH ₂ =CHCH ₂ NH ₂	38 (58)	39 (29)
33	CH ₃ (CH ₂) ₃ NH ₂	40 (58)	41 (16)
33		42 (57)	43 (14)
33	CH ₃ OH	44 (54)	45 (28)
33	PhCH ₂ OH	46 (48)	—
33	PhCH ₂ SH	47 (45)	48 (27)
34 (6-OH)	PhCH ₂ NH ₂ ^a	49 (34)	—
35 (9-OH)	PhCH ₂ NH ₂ ^a	50 (57)	—

^a Reaction in 2-propanol without indium(III) chloride, InCl₃.**Table 5.** IC₅₀ Values of Pyran Ring Derivatives of Naphthoquinone IDO Inhibitors

compd	IC ₅₀ (μM)	compd	IC ₅₀ (μM)	compd	IC ₅₀ (μM)
23 ^a	0.214	40	0.130	46	1.09
24	0.247	41	0.082	47	3.45
33	4.95	42	1.10	48	2.12
36	0.055	43	0.361	51	4.34
37	0.252	44	0.976	52	0.512
38	0.186	45	3.96	53 ^b	1.50
39	0.183				

^a Natural product commonly referred to as dehydro-α-lapachone. ^b Natural product commonly referred to as α-lapachone.**Scheme 2**

with the more complex marine natural product. To begin, we synthesized and tested the simplified pyranonaphthoquinone **23** (Table 5), where the tricyclic structure was found to restore essentially all the activity of annulin B. Notably, antitumor activity has been associated with compound **23**, which is also known as dehydro-α-lapachone.^{43,44} Incorporation of the ester from annulin B onto the pyran ring (**24**) had little effect on the potency of the pyranonaphthoquinone nucleus. However, reduction of the pyran ring (**51**) resulted in a dramatic loss in activity. Similarly, oxidation of the alkene to an epoxide (**33**) also dramatically reduced the activity of this tricyclic inhibitor. Based on the docking model of **23** (Figure 3b) and the hypothesized exposure of the pyran ring to solvent, we expected elaboration of the pyran ring to be permissible and therefore analyzed a selection of compounds with functionalized pyran rings. We found the most potent of these pyran ring derivatives to be 1,2-amino-alcohol derivatives (i.e., **36** and **41**). The absence of consistent differences between the cis and trans diastereomers

Table 6. IC₅₀ Values of Benzene Ring Derivatives of Naphthoquinone IDO Inhibitors

compd	IC ₅₀ (μM)	compd	IC ₅₀ (μM)
25	0.190	29	2.05
26	2.13	30	0.933
27	5.52	31 ^a	0.121
28	3.02	32	2.92

^a Natural product commonly referred to as α-caryopterone.

supports the notion that the region of the IDO enzyme occupied by these groups is not constrained, such as found at the opening of the active site.

Evaluation of Benzene Ring Derivatives. The study of the benzene ring of annulin B focused on the position and the nature of the oxygen substituent which was viewed as the most important functionality for intermolecular interactions in the active site. A distinct preference was observed with the C-6- and C-9 hydroxy-substituted pyranonaphthoquinones **25** and **31**, demonstrating between 5- and 45-fold greater potency than the other oxygen-substituted annulin B derivatives (Table 6). Nevertheless, the activity of **25** and **31** is roughly equal to that of the unsubstituted parent compound **23**. Consequently, the C-6 or C-9 hydroxyl substitution is permissible but does not appear to lead to any favorable interaction with IDO. Conversely, larger substitution in C-6 or C-9 or substituents in C-7 or C-8 clearly have a detrimental effect, probably due to steric interactions.

After an exploration of the optimal elements in the pyran ring (Table 5) and the benzene ring (Table 6), we synthesized two inhibitors (**49** and **50**) that combined the best elements of both ring substitutions. These compounds were also highly potent with IC₅₀'s of 0.058 and 0.059, respectively, thereby demonstrating that substitution is permitted in both rings. Although the substitution pattern of annulin B suggested this was possible, it was not to the extent demonstrated with the benzyl amine in **49** and **50**.

Further Evaluation of Most Active Inhibitors. Three of the most potent pyranonaphthoquinone derivatives, based on IC₅₀ values, were further analyzed to determine their inhibition constants and mode of inhibition. The inhibition constants for **36**, **41**, and **50** were determined to be 70, 61, and 66 nM, respectively. All three are more potent than annulin B (*K_i* = 120 nM^{20,21}) and thus represent the highest potency IDO inhibitors reported to date. Each of these compounds is also roughly 500-fold more potent than the most commonly employed IDO inhibitor 1MT. Interestingly, all three compounds exhibited reversible uncompetitive kinetics of inhibition (Supporting Information). Preincubation of three pyranonaphthoquinones (**31**, **36**, and **41**) with IDO failed to demonstrate any irreversible inhibition.

Due to the surprising activity of the hydroquinone derivative **14**, we attempted to generate and evaluate a hydroquinone derivative of one of the potent pyranonaphthoquinone derivatives. However, the rapid aerobic oxidation of each compound tested precluded analysis of the inhibitory activity of the hydroquinone form. Evaluation of the effect of the isolated enzyme assay reduction system (ascorbic acid/methylene blue) on these pyranonaphthoquinones did reveal evidence of hydroquinone formation (data not shown). Consequently, it is likely that both forms are present under the normal assay conditions, and it is possible that both are relevant to IDO inhibition as was witnessed with **13** and **14**.

Analysis of compounds **31**, **36**, and **41** in the same cell-based assay used to analyze menadione showed an attenuation of their activity versus the isolated enzyme assay (Table 7). However, unlike menadione which demonstrated clear cellular cytotoxicity

Table 7. IC₅₀ Values of Pyranonaphthoquinones Tested in Cell-Based Assay

compd	IC ₅₀ (μ M)
31	69
36	6.8
41	87

(Figure 2a), compounds **31**, **36**, and **41** demonstrated minimal impact on cell viability at 100 μ M after 24 h. Future studies will endeavor to improve the cell-based activity of the pyranonaphthoquinones.

Discussion

Focusing on the naphthoquinone core of the complex natural product annulin B, we have identified commercially available compounds with naphthoquinone core structures that display potent IDO inhibitory activity. Notably, some of these compounds were up to \sim 100-fold more potent than the commonly used IDO inhibitor 1MT. Reinforcing the definition of this series as a potentially important class of IDO inhibitors, the majority of high potency hits identified in a recently conducted screen of the NCI compound collection included either a naphthoquinone core or mimetic (unpublished results). We have established the applicability of IDO inhibition by compounds in this structural class to cancer treatment through *in vivo* evaluation of the representative bioactive compound menadione and followed with the development of novel pyranonaphthoquinone-based IDO inhibitors exhibiting submicromolar potencies produced from commercially available materials in a short number of synthetic steps.

Although the antitumor properties of menadione have long been recognized, this is the first report to demonstrate that IDO inhibition is an important mechanism of action. Previous studies of menadione antitumor activity have focused on oxidative stress as the primary mechanism of action. Intracellular redox cycling of menadione is catalyzed by bioreductive enzymes such as NAD(P)H:quinone oxidoreductase 1 (NQO1), NRH:quinone oxidoreductase 2 (NQO2), and cytochrome P450 reductase. Additional studies have also implicated nitric oxide synthases,⁴⁵ which are potentially interesting insofar as NO is known to directly antagonize IDO activity.⁴⁶ Depletion of glutathione (GSH) through direct conjugate formation and active export has also been proposed as a mechanism for menadione-mediated cytotoxicity.⁴⁷ More recently, menadione has been suggested to act by disrupting signaling pathways as an alternative to biochemical cytotoxic mechanisms.²⁹ In particular, treatment with menadione has been correlated with changes in the expression of molecules involved in controlling cell cycle progression.⁴⁸ All of these proposed mechanisms of action are based on the assumption that the antitumor activity of menadione is mediated through direct cytotoxicity to the tumor target. However, we have demonstrated here that the dramatic suppression of B16-F10 tumor growth that was elicited by menadione treatment in wild type mice was completely abolished in T cell-deficient nude mice. These data argue against direct cytotoxicity as the operative mechanism of action, instead implying that a T cell dependent, immune-mediated mechanism is crucial to the antitumor activity of menadione. In the B16-F10 tumor model, IDO is expressed not in the melanoma-derived tumor cells but rather in highly toleragenic, plasmacytoid dendritic cells (pDCs) within the tumor-draining lymph nodes.³³ Since the antitumor activity of menadione was also abolished in tumor-bearing, IDO nullizygous mice, where no IDO was present in the system, it is also evident that menadione must

inhibit IDO in order to manifest antitumor activity, providing genetic validation of the concept that IDO is an essential target of menadione.

Ingested phyloquinone (vitamin K1 produced by plants) is substantially converted to circulating menadione in humans.⁴⁹ As a vitamin K precursor, circulating menadione may be a significant source of menaquinone biosynthesis (vitamin K2 produced by bacteria and animals) in extra-hepatic tissues through uptake and prenylation. It remains to be determined whether levels of menadione achieved through dietary intake or supplementation of vitamin K are sufficient to have a meaningful effect on IDO activity. In a mouse lung tumor isograft model in which menaquinone supports metastasis through its role in the coagulation system (e.g., by impacting Factor X activation⁵⁰), the pro-metastatic effect of menaquinone can be combated with compounds that target the regenerative vitamin K cycle such as warfarin, which inhibits the enzyme vitamin K epoxide reductase. Interestingly, warfarin has also been shown to block both the *in vitro* and *in vivo* conversion of menadione to menaquinone.^{51,52} Taken together, this suggests that by inhibiting the conversion of endogenous menadione to menaquinone, anticoagulants could potentially leverage IDO inhibition by menadione while concomitantly interfering with the ability of menaquinone to support metastasis. Given the importance of both immune escape and metastasis in the pathophysiology of advanced cancers, further study in this area seems warranted.

One concern regarding the proposed mechanism of action of menadione was how the metabolism of this compound might affect its ability to inhibit IDO in cells. Menadione is sufficiently hydrophilic to be soluble in aqueous solution, but it also is sufficiently hydrophobic to diffuse across the plasma membrane.⁵³ Once menadione has entered a cell, it is rapidly conjugated to glutathione through nucleophilic addition to form **13** (quinone form) and **14** (hydroquinone form), which are no longer cell permeable and in fact are actively transported out of the cell.^{30,54} Nevertheless, we found that the menadione–glutathione conjugated compounds **13** and **14** were no less potent inhibitors of IDO than menadione itself despite the large size of the conjugated glutathione moiety. Since **13/14** are actively transported out of the cell, counteracting this (e.g., by inhibiting the ATP-dependent pump responsible for removing glutathione-conjugated menadione) might increase intracellular retention, thereby lowering the effective antitumor dose and perhaps also mitigating glutathione depletion (a side effect implicated in endothelial barrier damage³¹). Although the synthetic inhibitors reported in this study can also undergo redox cycling similar to menadione, they are chemically incapable of conjugation with glutathione since they are tetra-substituted quinones.⁵⁵ Consequently, glutathione processing is irrelevant to the cellular chemistry of the pyranonaphthoquinone-based IDO inhibitors.

In this study, we have identified the pyranonaphthoquinone moiety as the IDO inhibitory pharmacophore in the complex natural product annulin B, but the mechanism by which this structure achieves inhibition remains somewhat unclear. The quinone core is clearly important for IDO inhibition and the quinone oxygen may be the iron-binding group seen in previous inhibitor designs, most notably β -carboline, 4-phenylimidazole, and dithiocarbamates. Quinones are one of nature's privileged structures, performing essential roles as biological oxidants, e.g. vitamin K, vitamin E, ubiquinone, and plastoquinone. The unique nature of IDO as an oxidoreductase that is inactive in the ferric state and its sensitivity to inhibition by H₂O₂,^{56,57} combined with the oxidation potential of the quinone structure,

suggests that redox chemistry might be involved in the mechanism of inhibition. However, the absence of any correlation between inhibitor potency and the oxidation potential of the quinones (Table 1) tends to argue against such a mechanism as the primary basis for inhibition.

Indeed, the structure–activity relationships that we discovered in the preliminary screen (Table 1) and subsequent structural modifications (Tables 2–6) support a more complex interaction between IDO and the quinone-based inhibitors. Particularly intriguing in this regard is the potent IDO inhibitory activity exhibited by the menadione–glutathione conjugates **13** and **14** despite the fact that the hydroquinone could in theory replace ascorbic acid as a reductant, thereby activating IDO. There is strong evidence for phenols, such as in hydroquinone, to be monodentate ligands for iron,^{58–64} in line with speculation that iron binding by this moiety is important for IDO inhibition. One possible interpretation of this model is that the quinone **13** may be acting as a prodrug for the hydroquinone **14** since, presumably, under the assay conditions some of the quinone is reduced by ascorbic acid/methylene blue to the hydroquinone. This hypothesis is consistent with the observation that **14** is a more potent IDO inhibitor than **13**.

Future experiments will endeavor to understand the role of the quinone structure as well as redox chemistry in the inhibition of IDO. Based on the structure–activity relationships in the pyranonaphthoquinones, structural complementarity between the inhibitor and IDO clearly has an important role in inhibition as well. Moreover, computational docking predicted binding at the active site and rationalized many of the successful structural modifications. The uncompetitive mode of inhibition displayed by the most potent inhibitors (**34**, **39**, and **50**) would normally point to allosteric binding and regulation; however, other IDO inhibitors with a similar mode of inhibition have been shown to actually bind at the active site. Detailed kinetic analysis may shed further light on the precise molecular mechanism of IDO inhibition by this class of compounds. In addition, studies will also focus on enhancing the cell-based potency of this intriguing and highly potent class of IDO inhibitors.

Experimental Section

General Procedures. All reactants and reagents were commercially available and were used without further purification unless otherwise indicated. Anhydrous CH_2Cl_2 , benzene, and 2-propanol were obtained by distillation from calcium hydride under nitrogen. Anhydrous MeOH was obtained by distillation from Mg metal under nitrogen. All reactions were carried out under an inert atmosphere of argon or nitrogen unless otherwise indicated. Concentrated refers to the removal of solvent with a rotary evaporator at normal water aspirator pressure followed by further evacuation with a two-stage mechanical pump. Thin-layer chromatography was performed using silica gel 60 Å pre-coated glass or aluminum-backed plates (0.25 mm thickness) with fluorescent indicator, which were cut. Developed TLC plates were visualized with UV light (254 nm), iodine, or KMnO_4 . Flash column chromatography was conducted with the indicated solvent system using normal-phase silica gel 60 Å, 230–400 mesh. Yields refer to chromatographically and spectroscopically pure (>95%) compounds, except as otherwise indicated. All new compounds were determined to be >95% pure by NMR, HPLC, and/or GC as indicated. Melting points were determined using an open capillary and are uncorrected. ^1H and ^{13}C NMR spectra were recorded at 300 and 75 MHz, respectively. Chemical shifts are reported in δ values (ppm) relative to an internal reference (0.05% v/v) of tetramethylsilane (TMS) for ^1H NMR and the solvent peak in ^{13}C NMR, except where noted. Peak splitting patterns in the ^1H NMR are reported as follows: s, singlet; d, doublet; t, triplet; q, quartet; m, multiplet; br, broad. ^{13}C experiments with the attached proton

test (APT) sequence have multiplicities reported as δ_{u} (up) for methyl and methine and δ_{d} (down) for methylene and quaternary carbons. Normal-phase HPLC (NP-HPLC) analysis was performed with UV detection at 254 nm and a 5 μm silica gel column (250–4.6 mm) eluted with 90:10 or 85:15 *n*-hexane/IPA at 0.5 or 1 mL/min. Reversed-phase HPLC (RP-HPLC) analysis was performed with UV detection at 254 nm and a 5 μm Eclipse XDB-C₈ column (250–4.6 mm) eluted with 50:50 solvent A/solvent B; solvent A, 40% acetonitrile in water; solvent B, 0.1 M ammonium acetate adjusted to pH 5.3 with glacial acetic acid. IR data were obtained with an FT-IR spectrometer. MS data were recorded with atmospheric pressure chemical ionization (APCI) or atmospheric pressure electrospray ionization (APESI) mode.

(S)-2-Amino-5-((R)-1-(carboxymethylamino)-3-(3-methyl-1,4-dioxo-1,4-dihydronaphthalen-2-ylthio)-1-oxopropan-2-ylamino)-5-oxopentanoic Acid (13**).** Prepared according to the literature procedure⁶⁵ with a minor modification. To a solution of 2-methyl-1,4-naphthoquinone (200 mg, 1.16 mmol) in dimethyl sulfoxide (6 mL) and 95% ethanol (6 mL) at 0 °C was added L-glutathione (178 mg, 0.581 mmol) as a solution in water (2 mL). After the reaction mixture was stirred for 1 h, the reaction was diluted with ethyl acetate (50 mL) and filtered. The precipitate (220 mg) was boiled with water (30 mL) and filtered; the filtrate was diluted with ethanol (15 mL) and left undisturbed overnight. The precipitated product was isolated as a yellow solid (83 mg) in 30% yield, mp = 195–197 °C dec. The product has poor solubility in many solvents, which made it difficult to obtain NMR information: TLC R_f = 0.40 (30% $\text{H}_2\text{O}/\text{MeOH}$ with 0.1% $\text{CF}_3\text{CO}_2\text{H}$); ^1H NMR (CDCl_3 + TFA) δ 10.99 (s, 1H), 8.49–8.07 (m, 2H), 7.86–7.78 (m, 4H), 4.84 (dd, 1H, J = 5.55, 2.75 Hz), 4.35 (m, 1H), 4.19 (d, 2H, J = 1.02 Hz), 3.46 (dd, 1H, J = 8.55, 5.58 Hz), 3.34 (dd, 1H, J = 7.68, 6.3 Hz), 2.83–2.87 (m, 2H), 2.45–2.36 (m, 2H), 2.40 (s, 3H); ^{13}C NMR ($\text{DMSO}-d_6$) δ_{u} 134.4, 134.2, 126.9, 126.5, 53.6, 15.6 (2C); δ_{d} 182.3, 180.8, 172.5, 171.4, 171.0, 170.6, 148.3, 145.3, 132.8, 131.8, 41.5, 35.6, 31.8, 26.9; IR (KBr) 3353, 1682, 1642, 1511 cm^{-1} ; APESI-MS m/z 500 (M^+ + Na, 55), 478 (M^+ + 1, 100); RP-HPLC t_R = 6.14 min (50:50; solvent A/solvent B, 0.5 mL/min).

(S)-2-Amino-5-((R)-1-(carboxymethylamino)-3-(1,4-dihydroxy-3-methylnaphthalen-2-ylthio)-1-oxopropan-2-ylamino)-5-oxopentanoic Acid (14**).** Prepared according to the literature procedure⁶⁵ with a minor modification. To a solution of 2-methyl-1,4-naphthoquinone (100 mg, 0.581 mmol) under nitrogen in 95% ethanol (10 mL) at 0 °C was added L-glutathione (178 mg, 0.581 mmol) as a solution in water (2 mL). After being stirred overnight at rt, the precipitated product was filtered and washed with water. The crude product (210 mg) was boiled with water (2–20 mL) and filtered while hot to afford the product as a violet solid in 57% yield: mp = 216–217 °C dec; TLC R_f = 0.40 (30% $\text{H}_2\text{O}/\text{MeOH}$ with 0.1% $\text{CF}_3\text{CO}_2\text{H}$); ^1H NMR ($\text{DMSO}-d_6$) δ 8.51 (d, 1H, J = 7.35 Hz), 8.38 (s, 1H), 7.98–7.94 (m, 2H), 7.35–7.24 (m, 2H), 4.12 (m, 1H), 3.51 (d, 2H, J = 4.5 Hz), 3.32–3.25 (m, 1H), 2.90–2.74 (m, 2H), 2.33 (s, 3H), 2.22–2.07 (m, 2H), 1.82 (m, 2H); ^{13}C NMR ($\text{DMSO}-d_6$) δ_{u} 126.3, 124.7, 122.7, 121.9, 53.2, 52.8, 14.9; δ_{d} 172.2, 171.0, 170.8, 170.7, 148.8, 142.5, 127.1, 123.0, 122.1, 113.1, 41.2, 37.5, 31.5, 26.7; IR (KBr) 3410, 3350, 1687, 1629, 1512 cm^{-1} ; APESI-MS m/z 502 (M^+ + Na, 15), 480 (M^+ + 1, 100); RP-HPLC t_R = 6.06 min (50:50; solvent A/solvent B, 0.5 mL/min).

8-Methoxy-2-(phenylamino)-1,4-naphthoquinone. Prepared from 5-methoxy-1,4-naphthoquinone⁶⁶ according to the literature procedure⁶⁷ in 77% yield: mp = 150–151 °C (lit mp 152 °C); TLC R_f = 0.45 (10% $\text{MeOH}/\text{CHCl}_3$); ^1H NMR (CDCl_3) δ 7.78 (dd, 1H, J = 6.58, 1.11 Hz), 7.71–7.66 (m, 2H), 7.43–7.38 (m, 2H), 7.27–7.17 (m, 3H), 6.35 (s, 1H), 4.03 (s, 3H); ^{13}C NMR (CDCl_3) δ_{u} 136.3, 129.8, 125.7, 122.9, 119.2, 116.4, 102.0, 56.6; δ_{d} 183.7, 180.4, 160.4, 145.9, 137.9, 135.7, 118.3; IR (KBr) 3302, 3275, 1670, 1616 cm^{-1} .

2-Hydroxy-8-methoxy-1,4-naphthoquinone (22**⁶⁸).** A mixture of 8-methoxy-2-(phenylamino)-1,4-naphthoquinone (0.500 g, 1.79 mmol) was heated to reflux for 5 h in concd HCl (15 mL). The reaction mixture was allowed to cool to rt, diluted with water (20

mL), and extracted with CHCl_3 . The organic extract was dried (Na_2SO_4) and concentrated to afford a brownish solid: 325 mg in 89% yield; mp = 202–207 °C dec (lit.⁶⁸ mp = 211–214 °C dec; TLC R_f = 0.18 (10% MeOH/ CHCl_3); ^1H NMR (CDCl_3) δ 7.80–7.71 (m, 3H), 7.28 (d, 1H, J = 1.23 Hz), 6.29 (s, 1H), 4.04 (s, 3H); ^{13}C NMR (CDCl_3) δ_u 137.0, 119.7, 117.1, 108.7, 56.7; δ_d 184.9, 180.3, 160.6, 157.0, 135.5; IR (KBr) 3206, 1662 cm^{-1} .

2,8-Dihydroxy-1,4-naphthoquinone (21). Prepared from **22** according to the literature procedure⁶⁷ in 73% yield: mp = 214–216 °C dec (lit.⁶⁷ mp = 210–215 °C dec; TLC R_f = 0.33 (20% MeOH/ CHCl_3); ^1H NMR (CDCl_3 + CD_3OD) δ 7.67–7.57 (m, 2H), 7.21 (dd, 1H, J = 6.33, 1.62 Hz), 6.23 (s, 1H); ^{13}C NMR (CDCl_3 + CD_3OD) δ_u 137.2, 123.3, 118.7, 111.7; δ_d 185.9, 185.1, 161.3, 159.2, 132.4, 113.8.

General Procedure for the Synthesis of Pyranonaphthoquinones by the 6 π Electrocyclization Reaction. A solution of the appropriate 1,4-naphthoquinone (1.00 mmol) and α,β -unsaturated aldehyde (1.25 mmol), β -alanine (0.15 mmol), and acetic acid (6.0 mmol) in benzene (15 mL) was heated to reflux for 18 h. The reaction mixture was then concentrated *in vacuo*. Flash chromatography afforded the desired products.

2,2-Dimethyl-2H-benzof[*g*]chromene-5,10-dione (23). Pyranonaphthoquinone **23** was synthesized from 2-hydroxy-1,4-naphthoquinone **7** and 3-methylcrotonaldehyde according to the general procedure to yield 68%: mp = 142–143 °C (lit. mp = 145–146 °C). The product matched previously reported analytical data in the literature.⁴¹

Methyl 2-Methyl-5,10-dioxo-5,10-dihydro-2H-benzof[*g*]chromene-2-carboxylate (24). Pyranonaphthoquinone **24** was synthesized from 2-hydroxy-1,4-naphthoquinone **7** and fumaraldehydic acid methyl ester^{69,70} according to the general procedure to afford **24** as a yellow solid in 22% yield: mp = 131–132 °C; TLC R_f = 0.43 (20% EtOAc/hexanes); ^1H NMR (CDCl_3) δ 8.14–8.08 (m, 2H), 7.76–7.70 (m, 2H), 6.79 (d, 1H, J = 9.84 Hz), 5.88 (d, 1H, J = 9.84 Hz), 3.77 (s, 3H), 1.84 (s, 3H); ^{13}C NMR (CDCl_3) δ_u 134.3, 133.7, 126.6, 126.5, 126.2, 118.0, 53.3, 25.5; δ_d 181.8, 178.9, 170.8, 152.6, 131.6, 131.5, 117.9, 81.1; IR (KBr) 1749, 1671, 1651 cm^{-1} ; APCI-MS m/z 284 (M^+ , 100); NP-HPLC t_R = 7.1 min (85:15; *n*-hexane/IPA, 0.5 mL/min).

6-Hydroxy-2,2-dimethyl-2H-benzof[*g*]chromene-5,10-dione (25). Pyranonaphthoquinone **25** was synthesized from 2,5-dihydroxy-1,4-naphthoquinone **15**⁷¹ and 3-methylcrotonaldehyde according to the general procedure to afford **25** as an orange-red solid in 69% yield: mp = 159–160 °C (lit.⁷² mp = 156–158 °C); TLC R_f = 0.65 (20% EtOAc/hexanes); ^1H NMR (CDCl_3) δ 12.2 (s, 1H), 7.61 (dd, 1H, J = 6.18, 1.26 Hz), 7.53 (t, 1H, J = 8.22 Hz), 7.22 (dd, 1H, J = 7.08, 1.26 Hz), 6.60 (d, 1H, J = 10.02 Hz), 5.73 (d, 1H, J = 10.05 Hz), 1.56 (s, 6H); ^{13}C NMR (CDCl_3) δ_u 135.5, 130.9, 125.1, 119.3, 114.7, 28.6; δ_d 187.6, 179.3, 161.3, 153.2, 131.6, 117.7, 113.8, 81.1; IR (KBr) 3452, 1671, 1620 cm^{-1} ; APCI-MS m/z 258 (M^+ + 2, 15), 257 (M^+ + 1, 100); NP-HPLC t_R = 7.4 min (85:15; *n*-hexane/IPA, 0.5 mL/min).

6-Methoxy-2,2-dimethyl-2H-benzof[*g*]chromene-5,10-dione (26). Pyranonaphthoquinone **26** was synthesized from 2-hydroxy-5-methoxy-1,4-naphthoquinone **16**⁷¹ and 3-methylcrotonaldehyde according to the general procedure to afford **26** as a yellow solid in 76% yield: mp = 126–127 °C; TLC R_f = 0.45 (40% EtOAc/hexanes); ^1H NMR (CDCl_3) δ 7.78 (dd, 1H, J = 6.57, 1.08 Hz), 7.61 (t, 1H, J = 8.40 Hz), 7.30 (d, 1H, J = 9.90 Hz), 6.67 (d, 1H, J = 9.96 Hz), 5.72 (d, 1H, J = 9.99 Hz), 4.0 (s, 3H), 1.53 (s, 6H); ^{13}C NMR (CDCl_3) δ_u 134.3, 131.4, 119.2, 118.6, 116.0, 56.7, 28.4; δ_d 181.6, 180.2, 159.7, 150.8, 133.9, 119.5, 119.4, 79.9; IR (KBr) 1716, 1670, 1644 cm^{-1} ; APCI-MS m/z 271 (M^+ + 1, 25), 270 (M^+ , 100); NP-HPLC t_R = 11.8 min (85:15; *n*-hexane/IPA, 0.5 mL/min).

7-Hydroxy-2,2-dimethyl-2H-benzof[*g*]chromene-5,10-dione (27). Pyranonaphthoquinone **27** was synthesized from 2,6-dihydroxy-1,4-naphthoquinone **17**⁷³ and 3-methylcrotonaldehyde according to the general procedure to afford **27** as an orange-red solid in 71% yield: mp = 195 °C dec; TLC R_f = 0.50 (5% MeOH/ CHCl_3); ^1H NMR (CDCl_3 + CD_3OD) δ 7.96 (dd, 1H, J = 6.09, 2.40 Hz), 7.38

(d, 1H, J = 1.83 Hz), 7.05 (dd, 1H, J = 6.27, 2.19 Hz), 6.59 (dd, 1H, J = 7.89, 2.1 Hz), 5.67 (d, 1H, J = 9.99 Hz), 1.54 (s, 3H); ^{13}C NMR (CDCl_3 + CD_3OD) δ_u 130.3, 129.5, 120.2, 115.4, 112.7, 28.4; δ_d 182.6, 179.1, 163.2, 153.3, 134.0, 124.0, 117.5, 80.8. IR (KBr) 3343, 3246, 1738, 1660, 1630 cm^{-1} ; APCI-MS m/z 256 (M^+ , 15), 255 (M^+ – 1, 100); NP-HPLC t_R = 8.4 min (85:15; *n*-hexane/IPA, 0.5 mL/min).

7-Methoxy-2,2-dimethyl-2H-benzof[*g*]chromene-5,10-dione (28). Pyranonaphthoquinone **28** was synthesized from 2-hydroxy-6-methoxy-1,4-naphthoquinone **18**⁷³ and 3-methylcrotonaldehyde according to the general procedure to afford **28** as a yellow solid in 71% yield: TLC R_f = 0.43 (20% EtOAc/hexanes); ^1H NMR (CDCl_3) δ 8.02 (d, 1H, J = 8.61 Hz), 7.53 (s, 1H), 7.12 (dd, 1H, J = 6.06, 2.25 Hz), 6.63 (d, 1H, J = 9.96 Hz), 5.67 (d, 1H, J = 9.99 Hz), 3.93 (s, 3H), 1.54 (s, 6H); ^{13}C NMR (CDCl_3) δ_u 130.4, 129.0, 119.4, 115.7, 110.4, 56.1, 28.6; δ_d 181.9, 179.1, 164.6, 153.1, 134.1, 125.2, 117.7, 80.7; IR (KBr) 1663, 1646 cm^{-1} ; APCI-MS m/z 272 (M^+ + 2, 20), 271 (M^+ + 1, 100); NP-HPLC t_R = 8.4 min (90:10; *n*-hexane/IPA, 0.5 mL/min).

8-Hydroxy-2,2-dimethyl-2H-benzof[*g*]chromene-5,10-dione (29). Pyranonaphthoquinone **29** was synthesized from 2,7-dihydroxy-1,4-naphthoquinone **19**⁷³ and 3-methylcrotonaldehyde according to the general procedure to afford a 75% yield of **29**, an orange-red solid: mp = 206–210 °C dec; TLC R_f = 0.50 (5% MeOH/ CHCl_3); ^1H NMR (CDCl_3) δ 7.94 (d, 1H, J = 8.46 Hz), 7.42 (d, 1H, J = 2.4 Hz), 7.10 (dd, 1H, J = 6.03, 2.43 Hz), 6.62 (d, 1H, J = 9.96 Hz), 5.74 (d, 1H, J = 9.99 Hz), 1.54 (s, 6H); ^{13}C NMR (CDCl_3 + CD_3OD) δ_u 131.2, 129.1, 120.9, 115.7, 112.6, 28.3; δ_d 181.7, 180.7, 162.3, 152.2, 133.5, 123.9, 118.0, 80.3; IR (KBr) 3354, 1673, 1638, 1570 cm^{-1} ; APCI-MS m/z 256 (M^+ , 20), 255 (M^+ – 1, 100); NP-HPLC t_R = 8.6 min (85:15; *n*-hexane/IPA, 0.5 mL/min).

8-Methoxy-2,2-dimethyl-2H-benzof[*g*]chromene-5,10-dione (30). Pyranonaphthoquinone **30** was synthesized from 2-hydroxy-7-methoxy-1,4-naphthoquinone **20**⁷³ and 3-methylcrotonaldehyde according to the general procedure to afford **30** as a yellow solid in 72% yield: mp = 130 °C. TLC R_f = 0.43 (20% EtOAc/hexanes); ^1H NMR (CDCl_3) δ 8.02 (d, 1H, J = 8.58 Hz), 7.53 (d, 1H, J = 2.31 Hz), 7.15 (dd, 1H, J = 6.09, 2.49 Hz), 6.64 (d, 1H, J = 9.96 Hz), 5.70 (d, 1H, J = 9.96 Hz), 3.93 (s, 3H), 1.54 (s, 6H); ^{13}C NMR (CDCl_3) δ_u 131.1, 128.8, 120.2, 115.9, 110.2, 56.1, 28.5; δ_d 181.5, 180.1, 163.9, 152.4, 133.7, 125.1, 118.0, 80.4. IR (KBr) 1673, 1641, 1595, 1578 cm^{-1} ; APCI-MS m/z 271 (M^+ + 1, 20), 270 (M^+ , 100); NP-HPLC t_R = 8.0 min (85:15; *n*-hexane/IPA, 0.5 mL/min).

9-Hydroxy-2,2-dimethyl-2H-benzof[*g*]chromene-5,10-dione (31). Pyranonaphthoquinone **31** was synthesized from 2,8-dihydroxy-1,4-naphthoquinone **21** and 3-methylcrotonaldehyde according to the general procedure to afford **31** as an orange solid in 56% yield: mp = 155–157 °C (lit.⁷² mp = 160–165 °C; lit.⁷⁴ mp = 143.5–145.5 °C dec); TLC R_f = 0.57 (25% EtOAc/hexanes); ^1H NMR (CDCl_3) δ 11.86 (s, 1H), 7.62–7.54 (m, 2H), 7.19 (dd, 1H, J = 5.70, 1.95 Hz), 6.61 (d, 1H, J = 10.02 Hz), 5.72 (d, 1H, J = 10.02 Hz), 1.55 (s, 6H); ^{13}C NMR (CDCl_3) δ_u 136.9, 131.5, 124.1, 119.2, 115.6, 28.6; δ_d 184.9, 181.2, 161.7, 152.3, 131.7, 118.7, 114.7, 80.9; IR (KBr) 3418, 1641, 1624, 1577 cm^{-1} ; APCI-MS m/z 257 (M^+ + 1, 15), 226 (M^+ , 100); NP-HPLC t_R = 7.5 min (85:15; *n*-hexane/IPA, 0.5 mL/min).

9-Methoxy-2,2-dimethyl-2H-benzof[*g*]chromene-5,10-dione (32). Pyranonaphthoquinone **32** was synthesized from 2-hydroxy-8-methoxy-1,4-naphthoquinone **22** and 3-methylcrotonaldehyde according to the general procedure to afford **32** as a yellow solid in 52% yield: mp 135–136 °C (lit.⁷⁵ mp = 139.5–141.5 °C; lit.⁷⁶ mp = 132–134 °C); TLC R_f = 0.40 (40% EtOAc/hexanes); ^1H NMR (CDCl_3) δ 7.75 (dd, 1H, J = 6.81, 0.78 Hz), 7.63 (t, 1H, J = 8.19 Hz), 7.23 (d, 1H, J = 8.43 Hz), 6.60 (d, 1H, J = 9.93 Hz), 5.65 (d, 1H, J = 9.93), 3.98 (s, 3H), 1.52 (s, 6H); ^{13}C NMR (CDCl_3) δ_u 135.2, 130.2, 119.2, 117.7, 115.5, 56.7, 28.5; δ_d 181.8, 178.8, 160.0, 153.5, 134.2, 119.6, 116.2, 80.6. IR (KBr) 1734, 1671, 1644, 1583 cm^{-1} ; APCI-MS m/z 272 (M^+ + 2, 15), 271 (M^+ + 1, 100); NP-HPLC t_R = 12.3 min (85:15; *n*-hexane/IPA, 0.5 mL/min).

2,2-Dimethyl-3,4-epoxy-2H-naphtho[2,3-*b*]pyran-5,10-dione (33). The compound was synthesized via the reported procedure⁴¹ to afford a 62% yield: mp = 138–139 °C (lit.⁴¹ mp 139–140 °C). The spectroscopic data matched the reported information in the literature.

5-Hydroxy-2,2-dimethyl-1aH-benzo[*g*]oxireno[2,3-*c*]chromene-4,9(2H,9bH)-dione (35). Alkene **31** (150 mg, 0.585 mmol) was dissolved in CH₂Cl₂, cooled to 0 °C, and treated with mCPBA (152 mg, 0.878 mmol).⁷⁷ The reaction was stirred overnight at 0 °C. The solvent was removed *in vacuo*, and the crude product was chromatographed on silica gel to afford 84 mg of the epoxide **35** (53% yield), a yellow solid. Unreacted **31** was also recovered (48 mg). Characterization data for **35**: mp = 145–150 °C; yellow solid; TLC *R_f* = 0.33 (20% EtOAc/hexanes); ¹H NMR (CDCl₃) δ 11.74 (s, 1H), 7.70–7.61 (m, 2H), 7.27–7.22 (m, 1H), 4.33 (d, 1H, *J* = 4.41 Hz), 3.55 (d, 1H, *J* = 4.44 Hz), 1.71 (s, 3H), 1.46 (s, 3H); ¹³C NMR (CDCl₃) δ_u 137.3, 124.3, 119.3, 61.6, 43.8, 25.3, 23.5; δ_d 184.1, 182.4, 162.1, 153.7, 131.9, 118.1, 114.5, 78.5; IR (KBr) 3421, 1644, 1612 cm⁻¹; APCI-MS *m/z* 305 (M⁺ + MeOH, 100), 273 (M⁺ + 1, 18).

General Procedure for the Epoxide-Opening Reaction. To a solution of epoxide **33** (256 mg, 1.0 mmol) in CH₂Cl₂ (10 mL) at 0 °C was added InCl₃ (0.05 mmol) followed by the addition of the appropriate nucleophile (4 equiv), and the reaction mixture was allowed to warm to rt and stirred for 1–3 h. The solvent was evaporated, and the crude product was chromatographed on silica to give the desired products. The relative stereochemical conformation was assigned based on the coupling constant of the methine protons in ¹H NMR and confirmed in the case of **34** by an X-ray crystal structure.

(3S,4S and 3R,4R)-4-(Benzylamino)-3-hydroxy-2,2-dimethyl-3,4-dihydro-2H-benzo[*g*]chromene-5,10-dione (36). Compound **36** was synthesized using the general procedure with benzylamine. Chromatographic separation afforded pure *cis* diastereomer **36** as a yellow solid in 53% yield: mp = 155 °C; TLC *R_f* = 0.30 (25% EtOAc/hexanes); ¹H NMR (CDCl₃) δ 8.07–8.01 (m, 2H), 7.72–7.63 (m, 2H), 7.45–7.25 (m, 5H), 4.66 (br s, 1H), 3.99–3.88 (m, 3H), 3.72 (d, 1H, *J* = 4.47 Hz), 3.32 (br s, 1H), 1.67 (s, 3H), 1.25 (s, 3H); ¹³C NMR (CDCl₃) δ_u 134.4, 133.5, 128.8, 128.5, 127.7, 126.6, 126.3, 66.9, 51.6, 24.8, 22.5; δ_d 185.7, 179.4, 155.0, 139.1, 132.4, 131.0, 117.3, 80.7, 51.9; IR (KBr) 3342, 1681, 1643, 1612, 1578 cm⁻¹; APCI-MS *m/z* 365 (M⁺ + 2, 25), 364 (M⁺ + 1, 100); NP-HPLC *t_R* = 7.6 min (85:15; *n*-hexane/IPA, 0.5 mL/min).

(3R,4S and 3S,4R)-4-(Benzylamino)-3-hydroxy-2,2-dimethyl-3,4-dihydro-2H-benzo[*g*]chromene-5,10-dione (37). Compound **37** was synthesized using the general procedure with benzylamine. Chromatographic separation afforded pure *trans* diastereomer **37** as a yellow solid in 37% yield: mp = 88–89 °C; TLC *R_f* = 0.50 (5% MeOH/CHCl₃); ¹H NMR (CDCl₃) δ 8.12–8.08 (m, 2H), 7.77–7.67 (m, 2H), 7.33–7.19 (m, 5H), 3.90 (d, 1H, *J* = 8.58 Hz), 3.79 (d, 1H, *J* = 8.55 Hz), 3.68 (d, 1H, *J* = 12.39 Hz), 3.53 (d, 1H, *J* = 12.36 Hz), 2.97 (br s, 1H), 1.65 (s, 3H), 1.31 (s, 3H); ¹³C NMR (CDCl₃) δ_u 134.4, 133.5, 128.7, 128.4, 127.4, 126.7, 126.3, 70.0, 55.3, 26.1, 19.3; δ_d 184.9, 179.6, 155.5, 140.0, 132.4, 131.3, 119.5, 82.2, 48.3; IR (KBr) 3343, 1723, 1683, 1640, 1607, 1577 cm⁻¹; APCI-MS *m/z* 365 (M⁺ + 2, 25), 364 (M⁺ + 1, 100); NP-HPLC *t_R* = 8.0 min (85:15; *n*-hexane/IPA, 0.5 mL/min).

(3S,4S and 3R,4R)-4-(Allylamino)-3-hydroxy-2,2-dimethyl-3,4-dihydro-2H-benzo[*g*]chromene-5,10-dione (38). Compound **38** was synthesized using the general procedure with allylamine. Chromatographic separation afforded pure *cis* diastereomer **38** as a yellow solid in 58% yield: mp = 127–128 °C; TLC *R_f* = 0.60 (5% MeOH/CHCl₃); ¹H NMR (CDCl₃) δ 8.10–8.04 (m, 2H), 7.76–7.66 (m, 2H), 6.06–5.93 (m, 1H), 5.31 (dd, 1H, *J* = 15.66, 1.51 Hz), 5.20 (dd, 1H, *J* = 8.97, 1.26 Hz), 3.94 (d, 1H, *J* = 4.53 Hz), 3.67 (d, 1H, *J* = 4.53 Hz), 3.43–3.40 (m, 2H), 1.67 (s, 3H), 1.28 (s, 3H); ¹³C NMR (CDCl₃) δ_u 135.9, 134.3, 133.4, 126.6, 126.3, 66.8, 51.3, 24.8, 22.5; δ_d 185.6, 179.3, 155.1, 132.5, 131.0, 117.4, 117.2, 80.7, 50.1; IR (KBr) 3355, 1681, 1641, 1609 cm⁻¹; APCI-MS *m/z* 315 (M⁺ + 2, 20), 314 (M⁺ + 1, 100); NP-HPLC *t_R* = 10.0 min (85:15; *n*-hexane/IPA, 0.5 mL/min).

(3R,4S and 3S,4R)-4-(Allylamino)-3-hydroxy-2,2-dimethyl-3,4-dihydro-2H-benzo[*g*]chromene-5,10-dione (39). Compound **39** was synthesized using the general procedure with allylamine. Chromatographic separation afforded pure *trans* diastereomer **39** as a yellow solid in 29% yield: mp = 131–132 °C; TLC *R_f* = 0.60 (10% MeOH/CHCl₃); ¹H NMR (CDCl₃) δ 8.12–8.06 (m, 2H), 7.77–7.67 (m, 2H), 5.94–5.81 (m, 1H), 5.18 (dd, 1H, *J* = 15.6, 1.53 Hz), 5.13 (dd, 1H, *J* = 8.91, 1.32 Hz), 3.88 (d, 1H, *J* = 8.64 Hz), 3.76 (d, 1H, *J* = 8.64 Hz), 3.20 (dd, 1H, *J* = 7.98, 5.70 Hz), 3.01 (dd, 1H, *J* = 7.59, 6.03 Hz), 1.65 (s, 3H), 1.32 (s, 3H); ¹³C NMR (CDCl₃) δ_u 136.3, 134.5, 133.6, 126.7, 126.3, 70.1, 54.9, 26.2, 19.2; δ_d 184.9, 179.5, 155.5, 132.3, 131.2, 119.2, 116.7, 82.3, 46.6; IR (KBr) 3319, 3149, 1678, 1634, 1621 cm⁻¹; APCI-MS *m/z* 315 (M⁺ + 2, 20), 314 (M⁺ + 1, 100); NP-HPLC *t_R* = 10.5 min (85:15; *n*-hexane/IPA, 0.5 mL/min).

(3S,4S)-4-(Butylamino)-3-hydroxy-2,2-dimethyl-3,4-dihydro-2H-benzo[*g*]chromene-5,10-dione (40). Compound **40** was synthesized using the general procedure with allylamine. Chromatographic separation afforded pure *cis* diastereomer **40** as a yellow solid in 58% yield: mp = 120–121 °C; TLC *R_f* = 0.60 (5% MeOH/CHCl₃); ¹H NMR (CDCl₃) δ 8.11–8.05 (m, 2H), 7.76–7.66 (m, 2H), 3.85 (d, 1H, *J* = 4.50 Hz), 3.70 (d, 1H, *J* = 4.50 Hz), 2.86–2.68 (m, 2H), 1.68 (s, 3H), 1.62–1.38 (m, 4H), 1.29 (s, 3H), 0.96 (t, 3H, *J* = 7.11 Hz); ¹³C NMR (CDCl₃) δ_u 134.4, 133.5, 126.6, 126.3, 67.0, 52.5, 24.9, 22.4, 14.2; δ_d 185.8, 179.5, 155.0, 132.5, 131.2, 117.3, 80.8, 47.6, 32.4, 20.6; IR (KBr) 3335, 3281, 1680, 1629, 1602, 1575 cm⁻¹; APCI-MS *m/z* 331 (M⁺ + 2, 25), 330 (M⁺ + 1, 100); NP-HPLC *t_R* = 10.07 min (85:15; *n*-hexane/IPA, 0.5 mL/min).

(3R,4S and 3S,4R)-4-(Butylamino)-3-hydroxy-2,2-dimethyl-3,4-dihydro-2H-benzo[*g*]chromene-5,10-dione (41). Compound **41** was synthesized using the general procedure with allylamine. Chromatographic separation afforded pure *trans* diastereomer **41** as a yellow solid in 16% yield: mp = 103–104 °C; TLC *R_f* = 0.60 (10% MeOH/CHCl₃); ¹H NMR (CDCl₃) δ 8.11–8.05 (m, 2H), 7.75–7.66 (m, 2H), 3.81 (d, 1H, *J* = 9.00 Hz), 3.72 (d, 1H, *J* = 8.97 Hz), 2.52–2.44 (m, 1H), 2.31–2.23 (m, 1H), 1.65 (s, 3H), 1.43–1.30 (m, 4H), 1.30 (s, 3H), 0.86 (t, 3H, *J* = 7.20 Hz); ¹³C NMR (CDCl₃) δ_u 134.4, 133.5, 126.7, 126.3, 69.9, 55.1, 26.3, 18.9, 14.1; δ_d 184.9, 179.6, 155.5, 132.4, 131.4, 119.6, 82.2, 43.2, 32.9, 20.5; IR (KBr) 3210, 1681, 1637, 1612 cm⁻¹; APCI-MS *m/z* 331 (M⁺ + 2, 20), 330 (M⁺ + 1, 100); NP-HPLC *t_R* = 9.8 min (85:15; *n*-hexane/IPA, 0.5 mL/min).

(3S,4S and 3R,4R)-3-Hydroxy-2,2-dimethyl-4-morpholino-3,4-dihydro-2H-benzo[*g*]chromene-5,10-dione (42). Compound **42** was synthesized using the general procedure with morpholine. Chromatographic separation afforded pure *cis* diastereomer **42** as a yellow solid in 57% yield: mp = 103–104 °C; TLC *R_f* = 0.44 (5% MeOH/CHCl₃); ¹H NMR (CDCl₃) δ 8.09 (d, 2H, *J* = 7.59 Hz), 7.77–7.69 (m, 2H), 3.67 (t, 4H, *J* = 4.47 Hz), 3.57 (s, 2H), 3.06 (m, 2H), 2.94 (s, 1H), 2.65–2.58 (m, 2H), 1.64 (s, 3H), 1.34 (s, 3H); ¹³C NMR (CDCl₃) δ_u 134.5, 133.4, 126.6, 71.7, 62.1, 26.4, 19.6; δ_d 184.9, 179.6, 155.9, 132.5, 131.1, 119.8, 81.9, 68.3, 50.7; IR (KBr) 3500, 2938, 2854, 2819, 1666, 1645, 1611, 1581 cm⁻¹; APCI-MS *m/z* 345 (M⁺ + 2, 20), 344 (M⁺ + 1, 100); NP-HPLC *t_R* = 13.3 min (85:15; *n*-hexane/IPA, 0.5 mL/min).

(3R,4S and 3S,4R)-3-Hydroxy-2,2-dimethyl-4-morpholino-3,4-dihydro-2H-benzo[*g*]chromene-5,10-dione (43). Compound **43** was synthesized using the general procedure with morpholine. Chromatographic separation afforded pure *trans* diastereomer **43** as a yellow solid in 14% yield: mp = 157–158 °C; TLC *R_f* = 0.70 (5% MeOH/CHCl₃); ¹H NMR (CDCl₃) δ 8.13–8.09 (m, 2H), 7.79–7.68 (m, 2H), 4.17 (s, 1H), 3.95 (d, 1H, *J* = 6.15 Hz), 3.73–3.64 (m, 5H), 2.99 (m, 2H), 2.73–2.66 (m, 2H), 1.51 (s, 3H), 1.44 (s, 3H); ¹³C NMR (CDCl₃) δ_u 134.5, 133.6, 126.8, 126.6, 70.6, 56.6, 26.4, 22.2; δ_d 185.1, 179.3, 155.9, 132.1, 131.2, 118.3, 81.5, 67.9, 52.8; IR (KBr) 3487, 2990, 2852, 1679, 1638, 1578 cm⁻¹; APCI-MS *m/z* 345 (M⁺ + 2, 25), 344 (M⁺ + 1, 100); NP-HPLC *t_R* = 13.1 min (85:15; *n*-hexane/IPA, 0.5 mL/min).

(3S,4S and 3R,4R)-3-Hydroxy-4-methoxy-2,2-dimethyl-3,4-dihydro-2H-benzo[g]chromene-5,10-dione (44). Compound **44** was synthesized using the general procedure with methanol as previously described in the literature.⁴¹ Chromatographic separation afforded pure *cis* diastereomer **44** in 54% yield: ¹H NMR (CDCl₃) δ 8.10–8.07 (m, 2H), 7.73–7.67 (m, 2H), 4.35 (d, 1H, *J* = 3.0 Hz), 3.91 (br s, 1H), 3.64 (s, 3H), 1.88 (br s, 1H), 1.55 (s, 3H), 1.50 (s, 3H). The analytical data matched the literature report.⁴¹

(3R,4S and 3S,4R)-3-Hydroxy-4-methoxy-2,2-dimethyl-3,4-dihydro-2H-benzo[g]chromene-5,10-dione (45). Compound **45** was synthesized using the general procedure with methanol as previously described in the literature.⁴¹ Chromatographic separation afforded pure *trans* diastereomer **45** in 28% yield: ¹H NMR (CDCl₃) δ 8.21–8.05 (m, 2H), 7.79–7.73 (m, 2H), 7.01 (d, 1H, *J* = 2.49 Hz), 4.29 (d, 1H, *J* = 4.89 Hz), 3.17 (s, 3H), 2.02 (d, 1H, *J* = 5.61 Hz), 1.49 (s, 3H), 1.44 (s, 3H). The analytical data matched the literature report.⁴¹

(3S,4S and 3R,4R)-4-(Benzyloxy)-3-hydroxy-2,2-dimethyl-3,4-dihydro-2H-benzo[g]chromene-5,10-dione (46). Compound **46** was synthesized using the general procedure with benzyl alcohol. Chromatographic separation afforded pure *trans* diastereomer **46** as a yellow solid in 48% yield: mp = 149–150 °C; TLC *R_f* = 0.30 (20% EtOAc/hexanes); ¹H NMR (CDCl₃) δ 8.05 (t, 2H, *J* = 7.50 Hz), 7.72–7.62 (m, 2H), 7.38–7.26 (m, 5H), 4.97 (d, 1H, *J* = 11.28 Hz), 4.84 (d, 1H, *J* = 11.30 Hz), 4.60 (d, 1H, *J* = 2.88 Hz), 3.85 (d, 1H, *J* = 2.94 Hz), 2.18 (s, 1H), 1.55 (s, 3H), 1.52 (s, 3H); ¹³C NMR (CDCl₃) δ 134.5, 133.3, 128.6, 128.1, 128.0, 126.6, 126.4, 72.4, 71.5, 24.0, 23.7; δ _d 184.4, 180.1, 154.0, 138.6, 132.5, 131.2, 118.4, 81.4, 74.0; IR (KBr) 3481, 1635, 1591 cm⁻¹; APCI-MS *m/z* 366 (*M*⁺ + 2, 10), 365 (*M*⁺ + 1, 35), 257 (100); NP-HPLC *t_R* = 8.3 min (85:15; *n*-hexane/IPA, 0.5 mL/min).

(3R,4S and 3S,4R)-4-(Benzylthio)-3-hydroxy-2,2-dimethyl-3,4-dihydro-2H-benzo[g]chromene-5,10-dione (47). Compound **47** was synthesized using the general procedure with benzyl mercaptan. Chromatographic separation afforded pure *cis* diastereomer **47** as a yellow solid in 45% yield: mp = 151 °C; TLC *R_f* = 0.30 (25% EtOAc/hexanes); ¹H NMR (CDCl₃) δ 8.06–8.01 (m, 2H), 7.72–7.61 (m, 2H), 7.41–7.15 (m, 5H), 4.30 (d, 1H, *J* = 13.08 Hz), 4.05 (d, 1H, *J* = 13.08 Hz), 3.65–3.58 (m, 2H), 2.32 (d, 1H, *J* = 3.96 Hz), 1.49 (s, 3H), 1.29 (s, 3H); ¹³C NMR (CDCl₃) δ 134.3, 133.3, 129.4, 128.9, 127.6, 126.5, 126.4, 74.5, 42.4, 25.5, 20.8; δ _d 183.9, 179.5, 153.2, 138.6, 132.6, 131.1, 121.4, 81.1, 38.8; IR (KBr) 3453, 1673, 1645, 1603, 1574 cm⁻¹; APCI-MS *m/z* 382 (*M*⁺ + 2, 25), 381 (*M*⁺ + 1, 100); NP-HPLC *t_R* = 7.5 min (85:15; *n*-hexane/IPA, 0.5 mL/min).

(3S,4S and 3R,4R)-4-(Benzylthio)-3-hydroxy-2,2-dimethyl-3,4-dihydro-2H-benzo[g]chromene-5,10-dione (48). Compound **48** was synthesized using the general procedure with benzyl mercaptan. Chromatographic separation afforded pure *trans* diastereomer **48** as a yellow solid in 27% yield: mp = 127–128 °C; TLC *R_f* = 0.46 (20% EtOAc/hexanes); ¹H NMR (CDCl₃) δ 8.15–8.07 (m, 2H), 7.77–7.66 (m, 2H), 7.45–7.26 (m, 5H), 4.26 (d, 1H, *J* = 12.69 Hz), 4.14 (d, 1H, *J* = 12.69 Hz), 4.09 (d, 1H, *J* = 6.15 Hz), 3.74 (dd, 1H, *J* = 6.15, 3.39 Hz), 2.88 (d, 1H, *J* = 9.57 Hz), 1.50 (s, 3H), 1.24 (s, 3H); ¹³C NMR (CDCl₃) δ 134.4, 133.5, 129.5, 129.1, 127.9, 126.7, 126.5, 69.6, 42.6, 26.5, 20.3; δ _d 183.8, 179.6, 152.9, 138.1, 132.5, 131.2, 121.8, 81.7, 40.2; IR (KBr) 3421, 1681, 1645, 1609, 1574 cm⁻¹; APCI-MS *m/z* 382 (*M*⁺ + 2, 25), 381 (*M*⁺ + 1, 100); NP-HPLC *t_R* = 8.0 min (85:15; *n*-hexane/IPA, 0.5 mL/min).

(3S,4S)-4-(Benzylamino)-3,6-dihydroxy-2,2-dimethyl-3,4-dihydro-2H-benzo[g]chromene-5,10-dione (49). Alkene **25** (50 mg, 0.195 mmol) was dissolved in CH₂Cl₂ (3 mL), cooled to 0 °C, and treated with mCPBA (50.0 mg, 0.290 mmol).⁷⁷ The reaction was stirred overnight at 0 °C. The solvent was removed *in vacuo*, and the crude solid epoxide product **34** was treated with benzylamine (0.975 mmol) in 2-propanol (3 mL). After the reaction was stirred for 30 min, the solvent was removed *in vacuo*, and the crude was purified by preparative TLC to afford 25 mg of product **49** in 34% yield: TLC *R_f* = 0.30 (25% EtOAc/hexanes); ¹H NMR (CDCl₃) δ 12.27 (s, 1H), 7.64–7.22 (m, 8H), 4.01–3.90 (m, 3H), 3.72 (d, 1H,

J = 4.21 Hz), 1.67 (s, 3H), 1.26 (s, 3H); ¹³C NMR (CDCl₃) δ 135.6, 128.9, 128.5, 127.8, 125.5, 119.6, 66.9, 51.4, 24.8, 22.6; δ _d 191.5, 161.4, 155.9, 139.0, 131.1, 116.9, 81.2, 52.0; APCI-MS *m/z* 381 (*M*⁺ + 2, 20), 380 (*M*⁺ + 1, 100); NP-HPLC *t_R* = 4.0 min (85:15; *n*-hexane/IPA, 1 mL/min).

(3S,4S)-4-(Benzylamino)-3,9-dihydroxy-2,2-dimethyl-3,4-dihydro-2H-benzo[g]chromene-5,10-dione (50). To a solution of epoxide **35** (50 mg, 0.184 mmol) in 2-propanol (5 mL) at rt was added benzylamine (0.734 mmol), and the reaction mixture was stirred for 30 min. The solvent was removed *in vacuo*, and the crude was chromatographed on silica gel to afford the desired *cis* isomer **50** as a yellow solid (40 mg, 58% yield): mp = 140–141 °C; TLC *R_f* = 0.30 (20% EtOAc/hexanes); ¹H NMR (CDCl₃) δ 11.70 (s, 1H), 7.59–7.18 (m, 8H), 3.99–3.88 (m, 3H), 3.71 (d, 1H, *J* = 4.26 Hz), 1.67 (s, 3H), 1.26 (s, 3H); ¹³C NMR (CDCl₃) δ 137.1, 128.9, 128.6, 127.8, 124.0, 119.2, 66.9, 51.7, 24.9, 22.6; δ _d 184.8, 184.2, 161.9, 154.8, 139.0, 132.5, 118.1, 114.2, 81.0, 51.9; IR (KBr) 3340, 1636, 1603 cm⁻¹; APCI-MS *m/z* 381 (*M*⁺ + 2, 25), 380 (*M*⁺ + 1, 100); NP-HPLC *t_R* = 7.8 min (85:15; *n*-hexane/IPA, 0.5 mL/min).

2,2-Dimethyl-3,4-dihydro-2H-benzo[g]chromene-5,10-dione (51). Prepared according to the literature procedure⁴¹ to afford 92% yield of **51**: mp = 114–115 °C (lit.⁴¹ mp = 113–114 °C); ¹H NMR (CDCl₃) δ 8.10–8.05 (m, 2H), 7.73–7.63 (m, 2H), 2.62 (t, 2H, *J* = 6.66 Hz), 1.83 (t, 2H, *J* = 6.60 Hz), 1.44 (s, 6H). The product matched previously reported analytical data in the literature.⁴¹

(3R,4S and 3S,4R)-3-Bromo-4-hydroxy-2,2-dimethyl-3,4-dihydro-2H-benzo[g]chromene-5,10-dione (52). Prepared according to the literature procedure⁴¹ to afford 26% yield of **52**: mp = 174–175 °C (lit.⁴¹ mp = 176 °C); ¹H NMR (CDCl₃) δ 8.14–8.09 (m, 2H), 7.79–7.72 (m, 2H), 5.09 (dd, 1H, *J* = 5.31, 1.62 Hz), 4.16 (d, 1H, *J* = 6.93 Hz), 4.04 (d, 1H, *J* = 1.5 Hz), 1.73 (s, 3H), 1.58 (s, 3H). The product matched previously reported analytical data in the literature.⁴¹

(3S,4S and 3R,4R)-3,4-Dihydroxy-2,2-dimethyl-3,4-dihydro-2H-benzo[g]chromene-5,10-dione (53). Prepared according to the literature procedure⁴¹ to afford 53% yield of **53**: mp = 168–169 °C; TLC *R_f* = 0.20 (25% EtOAc/hexanes); ¹H NMR (CDCl₃) δ 8.12–8.06 (m, 2H), 7.77–7.68 (m, 2H), 5.01 (d, 1H, *J* = 4.47 Hz), 4.80 (s, 1H), 3.84 (d, 1H, *J* = 4.44 Hz), 3.12 (s, 1H), 1.63 (s, 3H), 1.37 (s, 3H); ¹³C NMR (CDCl₃) δ 134.5, 133.9, 126.9, 126.2, 70.1, 63.0, 23.9, 23.6; δ _d 187.2, 179.4, 154.1, 132.2, 131.3, 117.2, 82.0; NP-HPLC *t_R* = 9.9 min (85:15; *n*-hexane/IPA, 1 mL/min).

Biochemical Assays. Recombinant human IDO was expressed and purified as described.⁷⁸ The IC₅₀ inhibition assays were performed in a 96-well microtiter plate as described by Littlejohn et al.⁷⁸ with some modification. Briefly, the reaction mixture contained 50 mM potassium phosphate buffer (pH 6.5), 40 mM ascorbic acid, 400 μ g/mL catalase, 20 μ M methylene blue, and ~27 nM purified recombinant IDO per reaction. The reaction mixture was added to the substrate, L-tryptophan (L-Trp), and the inhibitor. The inhibitors were serially diluted in 3-fold increments ranging from 100 μ M to 1.69 nM, and the L-Trp was tested at 100 μ M (*K_m* = 80 μ M). The reaction was carried out at 37 °C for 60 min and stopped by the addition of 30% (w/v) trichloroacetic acid. The plate was incubated at 65 °C for 15 min to convert *N*-formylkynurenine to kynurenine and was then centrifuged at 1250g for 10 min. Lastly, 100 μ L of supernatant from each well was transferred to a new 96-well plate and mixed at equal volume with 2% (w/v) *p*-dimethylaminobenzaldehyde in acetic acid. The yellow color generated from the reaction with kynurenine was measured at 490 nm using a Synergy HT microtiter plate reader (Bio-Tek, Winooski, VT). The data were analyzed using Graph Pad Prism 4 software (Graph Pad Software Inc., San Diego, CA). For the *K_i* determinations of **36**, **41**, and **50**, tryptophan concentrations were varied from 25 to 200 μ M (*K_m* = 42 μ M), and inhibitor concentrations were varied between 3-fold above and below the calculated IC₅₀. Otherwise, reaction conditions were exactly as described above. Data were analyzed with the Enzyme Kinetics module in SigmaPlot version 10.

Cell-Based IDO Inhibition and Cytotoxicity Assays. T-REx cells containing an inducible human *INDO* cDNA⁷⁹ were seeded in a 96-well plate at a density of 20000 cells per well in 100 μ L of DMEM + 10% FBS. IDO expression was induced for 72 h by the addition of 100 μ L of media containing 20 ng/mL doxycycline. The media was then discarded, the wells rinsed once, and serial dilutions of menadione in 200 μ L of phenol red-free DMEM + 10% FBS was added in triplicate and incubated for 18 h. The reaction was stopped by the addition of 40 μ L of 50% (w/v) TCA to each well, and the cells were fixed by incubating for 1 h at 4 °C.

To Assess IDO Activity. Following the TCA fixation step, the supernatants were transferred to a round-bottomed 96-well plate and incubated at 65 °C for 15 min. The plates were then centrifuged at 1250g for 10 min, and 100 μ L of clarified supernatant was transferred to a new flat-bottomed 96-well plate and mixed at equal volume with 2% (w/v) *p*-dimethylaminobenzaldehyde in acetic acid. The yellow reaction was measured at 490 nm using a Synergy HT microtiter plate reader (Bio-Tek, Winooski, VT).

To Assess Cell Viability. The TCA-fixed cells remaining in the 96-well plate following transfer of the media were processed essentially as described.⁸⁰ Fixed cells were washed four times in tap water, blotted, air-dried, and treated for 15 min at room temperature with 100 μ L of 0.4% (w/v) sulfarhodamine B (SRB) (Sigma-Aldrich, St. Louis, MO) prepared in 1% acetic acid. Wells were then rinsed four times in 1% acetic acid, air-dried, and developed by adding 200 μ L of 10 mM unbuffered Tris-HCl and incubating for 15 min at room temperature with gentle shaking. Staining intensity, proportional to cell number, was determined by reading the absorbance at 570 nm on a plate reader. Data were collected and analyzed using Excel software (Microsoft).

Tumor Formation and Drug Response. FVB-strain MMTV-*Neu* transgenic mice were obtained from the Jackson Laboratory. C57BL/6 and athymic NCr-*nu/nu* (nude mice) were obtained from NCI-Frederick. IDO knockout mice have previously been described.⁸¹ Studies involving mice were approved by the institutional animal use committee of the Lankenau Institute for Medical Research. For autochthonous mammary gland tumor treatment studies, parous, FVB-strain MMTV-*Neu* mice expressing the wild type form of the rat *HER2/Neu* proto-oncogene were used as described.¹⁴ B16-F10 melanoma-derived cell line isograft tumor challenge experiments were carried out as described.⁴ Menadione administered to mice as a single agent at the nonlethal dose of 25 mg/kg q.d. did not result in any appreciable change in body weight over the treatment period. The combination of menadione + paclitaxel administered to MMTV-*Neu* mammary gland tumor-bearing mice did result in average weight loss of ~8%, however, a comparable degree of weight loss was observed in the taxol-alone treatment cohort and there was no indication that this was further exacerbated by menadione treatment. Graphing and statistical analysis of the data was performed using Prism 4 software (GraphPad Software Inc., San Diego, CA).

Computational Methods. Small Molecule Preparation. Molecules were constructed in MOE (MOE Molecular Operating Environment Chemical Computing Group, version 2005.06 Montreal Canada <http://www.chemcomp.com/>) and ionized using MOE's WashMDB function, and hydrogens were added. The small molecule conformation was minimized to a gradient of 0.01 in the MMFF94x force field^{82,83} using a distance-dependent dielectric constant of 1.

Protein Preparation. Using the IDO crystal structure (PDB code 2D0T), hydrogen atoms were added, and tautomeric states and orientations of Asn, Gln, His residues were determined with Molprobit (http://molprobit.biochem.duke.edu/).^{84,85} Hydrogens were added to crystallographic waters using MOE (MOE Molecular Operating Environment Chemical Computing Group, version 2005.06 Montreal Canada <http://www.chemcomp.com/>). The Amber99⁸⁶ force field in MOE was used, and iron was parametrized in the Fe³⁺ state. Dioxygen was not added to the iron. All hydrogens were minimized to an rms gradient of 0.01 holding the remaining heavy atoms fixed. A stepwise minimization followed for all atoms

using a quadratic force constant (100) to tether the atoms to their starting geometries; for each subsequent minimization, the force constant was reduced by a half-until zero.

Docking Calculations. The 2-[*N*-cyclohexylamino]ethanesulfonic acid and 4-phenyl-1-imidazole ligands were removed from the active site prior to docking. Preliminary docking calculations performed with annulin B were carried out using MolDock.⁸⁷ Gold (version 3.1)^{88,89} and AutoDock (version 3.05)⁹⁰ were used with default parameters and reproduced the crystallographic position of 4-phenyl-1-imidazole binding to the heme. Docking of the naphthoquinone series of compounds using AutoDock and Gold produced a top scoring binding pose with a ketone oxygen within coordination distance to the heme iron.

Acknowledgment. We thank Ms. Erika Sutanto-Ward for excellent technical assistance. Dr. Mike McLeish of the University of Michigan is gratefully acknowledged for guidance with the enzyme inhibition kinetics analysis. We are also grateful to Dr. Andrew Mellor for generously providing IDO knockout mice used in this study. Financial support for this work was provided by the National Institutes of Health (NCI R01 CA109542). A.J.M. is also the recipient of grants from the DoD Breast Cancer Research Program (BC044350), the State of Pennsylvania Department of Health (CURE/Tobacco Settlement Award), the Lance Armstrong Foundation, and the Concern Foundation. G.C.P. is the recipient of NIH Grant Nos. CA82222 and CA100123. Additional support for this project was provided by grants to G.C.P. from the Charlotte Geyer Foundation and the Lankenau Hospital Foundation.

Supporting Information Available: Copies of ¹H and ¹³C NMR spectra and liquid chromatograms for compounds **13**, **14**, **24–32**, **36–43**, **46–50**, and **53**. Copies of ¹H and ¹³C NMR spectra for **35**. Copies of ¹H NMR spectra for previously synthesized compounds **45**, **51**, and **52**. X-ray crystal structure of **36** and Hanes–Woolf plots for **36**, **41**, and **50**. This material is available free of charge via the Internet at <http://pubs.acs.org>.

References

- (1) Dunn, G. P.; Bruce, A. T.; Ikeda, H.; Old, L. J.; Schreiber, R. D. Cancer immunoediting: from immunosurveillance to tumor escape. *Nat. Immunol.* **2002**, *3*, 991–8.
- (2) Mellor, A. L.; Munn, D. H. IDO expression by dendritic cells: tolerance and tryptophan catabolism. *Nat. Rev. Immunol.* **2004**, *4*, 762–74.
- (3) Muller, A. J.; Scherle, P. A. Targeting the mechanisms of tumoral immune tolerance with small-molecule inhibitors. *Nat. Rev. Cancer* **2006**, *6*, 613–625.
- (4) Hou, D. Y.; Muller, A. J.; Sharma, M. D.; DuHadaway, J.; Banerjee, T.; Johnson, M.; Mellor, A. L.; Prendergast, G. C.; Munn, D. H. Inhibition of indoleamine 2,3-dioxygenase in dendritic cells by stereoisomers of 1-methyl-tryptophan correlates with antitumor responses. *Cancer Res.* **2007**, *67*, 792–801.
- (5) Muller, A. J.; Malachowski, W. P.; Prendergast, G. C. Indoleamine 2,3-dioxygenase in cancer: targeting pathological immune tolerance with small-molecule inhibitors. *Expert Opin. Ther. Targets* **2005**, *9*, 831–49.
- (6) Sono, M.; Roach, M. P.; Coulter, E. D.; Dawson, J. H. Heme-Containing Oxygenases. *Chem. Rev.* **1996**, *96*, 2841–2888.
- (7) Botting, N. P. Chemistry and Neurochemistry of the Kynurenine Pathway of Tryptophan Metabolism. *Chem. Soc. Rev.* **1995**, *24*, 401–12.
- (8) Sono, M.; Hayaishi, O. The Reaction Mechanism of Indoleamine 2,3-Dioxygenase. *Biochem. Rev.* **1980**, *50*, 173–81.
- (9) Sono, M.; Taniguchi, T.; Watanabe, Y.; Hayaishi, O. Indoleamine 2,3-dioxygenase. Equilibrium studies of the tryptophan binding to the ferric, ferrous, and CO-bound enzymes. *J. Biol. Chem.* **1980**, *255*, 1339–45.
- (10) Kobayashi, K.; Hayashi, K.; Sono, M. Effects of tryptophan and pH on the kinetics of superoxide radical binding to indoleamine 2,3-dioxygenase studied by pulse radiolysis. *J. Biol. Chem.* **1989**, *264*, 15280–3.
- (11) Cady, S. G.; Sono, M. 1-Methyl-DL-tryptophan, beta-(3-benzofuranyl)-DL-alanine (the oxygen analog of tryptophan), and beta-[3-benzothienyl]-DL-alanine (the sulfur analog of tryptophan) are competi-

- tive inhibitors for indoleamine 2,3-dioxygenase. *Arch. Biochem. Biophys.* **1991**, 291, 326–33.
- (12) Peterson, A. C.; Migawa, M. T.; Martin, M. J.; Hamaker, L. K.; Czerwinski, K. M.; Zhang, W.; Arend, R. A.; Fiset, P. L.; Ozaki, Y.; Will, J. A.; Brown, R.; Cook, J. M. Evaluation of functionalized tryptophan derivatives and related compounds as competitive inhibitors of indoleamine 2,3-dioxygenase. *Med. Chem. Res.* **1994**, 3, 531–544.
- (13) Gaspari, P.; Banerjee, T.; Malachowski, W. P.; Muller, A. J.; Prendergast, G. C.; DuHadaway, J.; Bennett, S.; Donovan, A. M. Structure-activity study of brassinin derivatives as indoleamine 2,3-dioxygenase inhibitors. *J. Med. Chem.* **2006**, 49, 684–92.
- (14) Muller, A. J.; DuHadaway, J. B.; Donover, P. S.; Sutaranto-Ward, E.; Prendergast, G. C. Inhibition of indoleamine 2,3-dioxygenase, an immunoregulatory target of the cancer suppression gene Bin1, potentiates cancer chemotherapy. *Nat. Med.* **2005**, 11, 312–9.
- (15) Benner, S. A. Enzyme Kinetics and Molecular Evolution. *Chem. Rev.* **1989**, 89, 789–806.
- (16) Fersht, A. R. Catalysis, binding and enzyme-substrate complementarity. *Proc. R. Soc. London B Biol. Sci.* **1974**, 187, 397–407.
- (17) Amirkhani, A.; Heldin, E.; Markides, K. E.; Bergquist, J. Quantitation of tryptophan, kynurenine and kynurenic acid in human plasma by capillary liquid chromatography-electrospray ionization tandem mass spectrometry. *J. Chromatogr. B Anal. Technol. Biomed. Life Sci.* **2002**, 780, 381–7.
- (18) Huengsborg, M.; Winer, J. B.; Gompels, M.; Round, R.; Ross, J.; Shahmanesh, M. Serum kynurenine-to-tryptophan ratio increases with progressive disease in HIV-infected patients. *Clin. Chem.* **1998**, 44, 858–62.
- (19) Laich, A.; Neurauder, G.; Widner, B.; Fuchs, D. More rapid method for simultaneous measurement of tryptophan and kynurenine by HPLC. *Clin. Chem.* **2002**, 48, 579–81.
- (20) Pereira, A.; Vottero, E.; Roberge, M.; Mauk, A. G.; Andersen, R. J. Indoleamine 2,3-dioxygenase inhibitors from the Northeastern Pacific Marine Hydroid *Garveia annulata*. *J. Nat. Prod.* **2006**, 69, 1496–9.
- (21) Brastianos, H. C.; Vottero, E.; Patrick, B. O.; Van Soest, R.; Matainaho, T.; Mauk, A. G.; Andersen, R. J. Exiguamine A, an indoleamine-2,3-dioxygenase (IDO) inhibitor isolated from the marine sponge *Neopetrosia exigua*. *J. Am. Chem. Soc.* **2006**, 128, 16046–7.
- (22) Shaikh, I. A.; Johnson, F.; Grollman, A. P. Streptonigrin. I. Structure-activity relationships among simple bicyclic analogues. Rate dependence of DNA degradation on quinone reduction potential. *J. Med. Chem.* **1986**, 29, 1329–40.
- (23) Conant, J. B.; Fieser, L. F. Reduction Potentials of Quinones. II. The Potentials of Certain Derivatives of Benzoquinone, Naphthoquinone and Anthraquinone. *J. Am. Chem. Soc.* **1924**, 46, 1858–1881.
- (24) Prince, R. C.; Dutton, P. L.; Bruce, J. M. Electrochemistry of ubiquinones, Menaquinones and plastoquinones in aprotic solvents. *Fed. Eur. Biochem. Soc. Lett.* **1983**, 160, 273–276.
- (25) Butler, J.; Hoey, B. M. The apparent inhibition of superoxide dismutase activity by quinones. *J. Free Radic. Biol. Med.* **1986**, 2, 77–81.
- (26) Mukherjee, T. One-electron reduction of juglone (5-hydroxy-1,4-naphthoquinone): a pulse radiolysis study. *Radiat. Phys. Chem.* **1987**, 29, 455–462.
- (27) Wilson, I.; Wardman, P.; Lin, T. S.; Sartorelli, A. C. One-electron reduction of 2- and 6-methyl-1,4-naphthoquinone bioreductive alkylating agents. *J. Med. Chem.* **1986**, 29, 1381–4.
- (28) Ilan, Y. A.; Czapski, G.; Meisel, D. The one-electron transfer redox potentials of free radicals. I. The oxygen/superoxide system. *Biochim. Biophys. Acta* **1976**, 430, 209–24.
- (29) Lamson, D. W.; Plaza, S. M. The anticancer effects of vitamin K. *Altern. Med. Rev.* **2003**, 8, 303–18.
- (30) Ross, D.; Thor, H.; Orrenius, S.; Moldeus, P. Interaction of menadione (2-methyl-1,4-naphthoquinone) with glutathione. *Chem. Biol. Interact.* **1985**, 55, 177–84.
- (31) McAmis, W. C.; Schaeffer, R. C., Jr.; Baynes, J. W.; Wolf, M. B. Menadione causes endothelial barrier failure by a direct effect on intracellular thiols, independent of reactive oxidant production. *Biochim. Biophys. Acta* **2003**, 1641, 43–53.
- (32) Banerjee, T.; DuHadaway, J. B.; Gaspari, P.; Sutaranto-Ward, E.; Munn, D. H.; Mellor, A. L.; Malachowski, W. P.; Prendergast, G. C.; Muller, A. J. A key in vivo antitumor mechanism of action of natural product-based brassinins is inhibition of indoleamine 2,3-dioxygenase. *Oncogene* advance online publication 2007 (DOI 10.1038/sj.onc.1210939).
- (33) Munn, D. H.; Sharma, M. D.; Hou, D.; Baban, B.; Lee, J. R.; Antonia, S. J.; Messina, J. L.; Chandler, P.; Koni, P. A.; Mellor, A. L. Expression of indoleamine 2,3-dioxygenase by plasmacytoid dendritic cells in tumor-draining lymph nodes. *J. Clin. Invest.* **2004**, 114, 280–90.
- (34) Sono, M.; Cady, S. G. Enzyme kinetic and spectroscopic studies of inhibitor and effector interactions with indoleamine 2,3-dioxygenase. I. Norharman and 4-phenylimidazole binding to the enzyme as inhibitors and heme ligands. *Biochemistry* **1989**, 28, 5392–5399.
- (35) Sugimoto, H.; Oda, S.; Otsuki, T.; Hino, T.; Yoshida, T.; Shiro, Y. Crystal structure of human indoleamine 2,3-dioxygenase: catalytic mechanism of O₂ incorporation by a heme-containing dioxygenase. *Proc. Natl. Acad. Sci. U.S.A.* **2006**, 103, 2611–6.
- (36) Eguchi, N.; Watanabe, Y.; Kawanishi, K.; Hashimoto, Y.; Hayaishi, O. Inhibition of Indoleamine 2,3-Dioxygenase and Tryptophan 2,3-Dioxygenase by beta-Carboline and Indole Derivatives. *Arch. Biochem. Biophys.* **1984**, 232, 602–609.
- (37) Castro, C. E.; Hathaway, G. M.; Havlin, R. Oxidation and Reduction of Iron Porphyrins and Hemoproteins by Quinone and Hydroquinones. *J. Am. Chem. Soc.* **1977**, 99, 8032–8039.
- (38) Yamashita, E.; Zhang, H.; Cramer, W. A. Structure of the Cytochrome b(6)f Complex: Quinone Analogue Inhibitors as Ligands of Heme c. (n). *J. Mol. Biol.* **2007**, 370, 39–52.
- (39) Baymann, F.; Giusti, F.; Picot, D.; Nitschke, W. The ci/bH moiety in the b6f complex studied by EPR: a pair of strongly interacting hemes. *Proc. Natl. Acad. Sci. U.S.A.* **2007**, 104, 519–24.
- (40) Lee, Y. R.; Lee, W. K. Efficient Synthesis of Biologically Interesting Dehydro-alpha-Lapachone and alpha-Lapachone. *Synth. Commun.* **2004**, 34, 4537–4543.
- (41) Lee, Y. R.; Choi, J. H.; Trinh, D. T. L.; Kim, N. W. A Concise Route for the Synthesis of Pyranonaphthoquinone Derivatives. *Synthesis* **2005**, 3026–3034.
- (42) Kopanski, L.; Karbach, D.; Selbitschka, G.; Steglich, W. Vesparion, ein Naphtho[2,3-b]pyrandon-Derivat aus dem Schleimpilz *Metatrichia vesparium* (Myxomycetes). *Liebigs Ann. Chem.* **1987**, 793–796.
- (43) Itoigawa, M.; Ito, C.; Tan, H. T. W.; Okuda, M.; Tokuda, H.; Nishino, H.; Furukawa, H. Cancer chemopreventive activity of naphthoquinones and their analogs from *Avicennia* plants. *Cancer Lett.* **2001**, 174, 135–139.
- (44) Planchon, S. M.; Wuerzberger-Davis, S. M.; Pink, J. J.; Robertson, K. A.; Bornmann, W. G.; Boothman, D. A. Bcl-2 protects against beta-lapachone-mediated caspase 3 activation and apoptosis in human myeloid leukemia (HL-60) cells. *Oncol. Rep.* **1999**, 6, 485–492.
- (45) Garner, A. P.; Paine, M. J.; Rodriguez-Crespo, I.; Chinje, E. C.; Ortiz De Montellano, P.; Stratford, I. J.; Tew, D. G.; Wolf, C. R. Nitric oxide synthases catalyze the activation of redox cycling and bioreductive anticancer agents. *Cancer Res.* **1999**, 59, 1929–34.
- (46) Samelson-Jones, B. J.; Yeh, S. R. Interactions between nitric oxide and indoleamine 2,3-dioxygenase. *Biochemistry* **2006**, 45, 8527–38.
- (47) Chang, M.; Shi, M.; Forman, H. J. Exogenous glutathione protects endothelial cells from menadione toxicity. *Am. J. Physiol.* **1992**, 262, L637–43.
- (48) Kuriyama, S.; Hitomi, M.; Yoshiji, H.; Nonomura, T.; Tsujimoto, T.; Mito, A.; Akahane, T.; Ogawa, M.; Nakai, S.; Deguchi, A.; Masaki, T.; Uchida, N. Vitamins K2, K3 and K5 exert in vivo antitumor effects on hepatocellular carcinoma by regulating the expression of G1 phase-related cell cycle molecules. *Int. J. Oncol.* **2005**, 27, 505–11.
- (49) Thijssen, H. H.; Vervoort, L. M.; Schurgers, L. J.; Shearer, M. J. Menadione is a metabolite of oral vitamin K. *Br. J. Nutr.* **2006**, 95, 260–6.
- (50) Fasco, M. J.; Eagan, G. E.; Wilson, A. C.; Gierthy, J. F.; Lincoln, D. L. Loss of metastatic and primary tumor factor X activator capabilities by Lewis lung carcinoma cells cultured in vitamin K-dependent protein deficient serum. *Cancer Res.* **1988**, 48, 6504–9.
- (51) Dialameh, G. H. Stereobiochemical aspects of warfarin isomers for inhibition of enzymatic alkylation of menaquinone-0 to menaquinone-4 in chick liver. *Int. J. Vitam. Nutr. Res.* **1978**, 48, 131–5.
- (52) Taggart, W. V.; Matschner, J. T. Metabolism of menadione-6,7-³H in the rat. *Biochemistry* **1969**, 8, 1141–6.
- (53) Watanabe, N.; Dickinson, D. A.; Liu, R. M.; Forman, H. J. Quinones and glutathione metabolism. *Methods Enzymol.* **2004**, 378, 319–40.
- (54) Mauzeroll, J.; Bard, A. J.; Owhadian, O.; Monks, T. J. Menadione metabolism to thiodione in hepatoblastoma by scanning electrochemical microscopy. *Proc. Natl. Acad. Sci. U.S.A.* **2004**, 101, 17582–7.
- (55) Mundy, R. Activation and Detoxification of Naphthoquinones by NAD(P)H: Quinone Oxidoreductase. In *Quinones and Quinone Enzymes*; Sies, H., Packer, L., Eds.; Elsevier Academic Press: San Diego, CA, 2004; Vol. 382, pp 364–380.
- (56) Ohnishi, T.; Hirata, F.; Hayaish, O. Indoleamine 2,3-dioxygenase. Potassium superoxide as substrate. *J. Biol. Chem.* **1977**, 252, 4643–7.
- (57) Poljak, A.; Grant, R.; Austin, C. J.; Jamie, J. F.; Willows, R. D.; Takikawa, O.; Littlejohn, T. K.; Truscott, R. J.; Walker, M. J.; Sachdev, P.; Smythe, G. A. Inhibition of indoleamine 2,3-dioxygenase activity by H₂O₂. *Arch. Biochem. Biophys.* **2006**, 450, 9–19.
- (58) Lanznaster, M.; Neves, A.; Bortoluzzi, A. J.; Assumpcao, A. M.; Vencato, I.; Machado, S. P.; Drechsel, S. M. Electronic effects of electron-donating and -withdrawing groups in model complexes for iron-tyrosine-containing metalloenzymes. *Inorg. Chem.* **2006**, 45, 1005–11.

- (59) Kanamori, D.; Yamada, Y.; Onoda, A.; Okamura, T.-a.; Adachi, S.; Yamamoto, H.; Ueyama, N. Structures and properties of octaethylporphinato. (phenolate)iron(III) complexes with NH--O hydrogen bonds: modulation of Fe-O bond character by the hydrogen bond. *Inorg. Chim. Acta* **2005**, *358*, 331-338.
- (60) Darensbourg, D. J.; Ortiz, C. G.; Billodeaux, D. R. Synthesis and structural characterization of iron(III) salen complexes possessing appended anionic oxygen donor ligands. *Inorg. Chim. Acta* **2004**, *357*, 2143-2149.
- (61) Nee, M. W.; Lindsay Smith, J. R. Axial ligand exchange of iron(III) tetramesitylporphyrin phenolate complexes. *J. Chem. Soc., Dalton Trans.: Inorg. Chem.* **1999**, 3373-3377.
- (62) Uno, T.; Hatano, K.; Nishimura, Y.; Arata, Y. Spectrophotometric and resonance Raman studies on the formation of phenolate and thiolate complexes of (octaethylporphinato)iron(III). *Inorg. Chem.* **1990**, *29*, 2803-2807.
- (63) Roe, A. L.; Schneider, D. J.; Mayer, R. J.; Pyrz, J. W.; Widom, J.; Que, L. X-ray absorption spectroscopy of iron-tyrosinate proteins. *J. Am. Chem. Soc.* **1984**, *106*, 1676-1681.
- (64) Milburn, R. M. Iron(III)-Phenol Complexes. III. Enthalpies and Entropies of Iron(III)-Phenolate Associations. *J. Am. Chem. Soc.* **1967**, *89*, 54-58.
- (65) Nickerson, W. J.; Falcone, G.; Strauss, G. Studies on Quinone-Thioethers. I. Mechanism of Formation and Properties of Thiodione. *Biochemistry* **1963**, *2*, 537-543.
- (66) Tietze, L. F.; Güntner, C.; Gericke, K. M.; Schuberth, I.; Bunkoczi, G. A Diels-Alder Reaction for the Total Synthesis of the Novel Antibiotic Antitumor Agent Mensacarcin. *Eur. J. Org. Chem.* **2005**, 2459-2467.
- (67) MacLeod, J. W.; Thomson, R. H. Studies in the Juglone Series. IV. The Addition of Aniline and Toluene-p-thiol to 5-Substituted 1,4-Naphthoquinones. *J. Org. Chem.* **1960**, *25*, 36-42.
- (68) Ameer, F.; Giles, R. G. F.; Green, I. R.; Pearce, R. Synthesis of Methoxy-2-hydroxy-1,4-naphthoquinones and Reaction of One Isomer with Aldehydes Under Basic Conditions. *Synth. Commun.* **2004**, *34*, 1247-1258.
- (69) Wolff, M.; Seemann, M.; Grosdemange-Billiard, C.; Tritsch, D.; Campos, N.; Rodríguez-Concepción, M.; Boronat, A.; Rohmer, M. Isoprenoid biosynthesis via the methylerythritol phosphate pathway. (E)-4-Hydroxy-3-methylbut-2-enyl diphosphate: chemical synthesis and formation from methylerythritol cyclodiphosphate by a cell-free system from *Escherichia coli*. *Tetrahedron Lett.* **2002**, *43*, 2555-2559.
- (70) Ishida, A.; Mukaiyama, T. Total Synthesis of (±)Variotin and Its Analogs. *Bull. Chem. Soc. Jpn.* **1978**, *51*, 2077-2081.
- (71) Lothar, K.; Doris, K.; Gerhard, S.; Wolfgang, S. Fungal pigments. 53. Vesparione, a naphtho[2,3-b]pyrandione derivative from the slime mold *Metatrichia vesparium* (Myxomycetes). *Liebigs Ann. Chem.* **1987**, 793-796.
- (72) De Oliveira, A. B.; Ferreira, D. T.; Raslan, D. S. Synthesis of the naturally occurring naphtho[2,3-b]pyran-5,10-quinones α -caryopterone, dihydro- α -caryopterone and their isomers, 6-hydroxydihydro- α -lapachone and 6-hydroxy- α -lapachone. *Tetrahedron Lett.* **1988**, *29*, 155-8.
- (73) Malerich, J. P.; Maimone, T. J.; Elliott, G. I.; Trauner, D. Biomimetic Synthesis of Antimalarial Naphthoquinones. *J. Am. Chem. Soc.* **2005**, *127*, 6276-6283.
- (74) Matsumoto, T.; Mayer, C.; Eugster, C. H. α -Caryopterone, a new Pyrano-juglone from *Caryopteris clandonensis*. *Helv. Chim. Acta* **1969**, *52*, 808-812.
- (75) Tapia, R.; Valderrama, J. A.; Quintanar, C. Synthesis of Naphtho[2,3-b]pyranoquinones and its Aza-analogues from a Useful Benzopyranoquinone Intermediate. *Heterocycles* **1994**, *38*, 1797-1804.
- (76) Giles, R. G. F.; Roos, G. H. P. Syntheses of the naturally occurring naphtho[2,3-b]pyran-5,10-quinones α -caryopterone, dihydro- α -caryopterone, and O-methyldihydro- α -caryopterone. *J. Chem. Soc., Perkin Trans. 1* **1976**, 1632-1635.
- (77) Burns, C. J.; Gill, M.; Saubern, S. Pigments of fungi. XXI. Synthesis of (±)-6-demethoxyaustrocortirubin. *Aust. J. Chem.* **1991**, *44*, 1427-1445.
- (78) Littlejohn, T. K.; Takikawa, O.; Skylas, D.; Jamie, J. F.; Walker, M. J.; Truscott, R. J. Expression and purification of recombinant human indoleamine 2, 3-dioxygenase. *Protein Expr. Purif.* **2000**, *19*, 22-9.
- (79) Metz, R.; Duhadaway, J. B.; Kamasani, U.; Laury-Kleintop, L.; Muller, A. J.; Prendergast, G. C. Novel tryptophan catabolic enzyme IDO2 is the preferred biochemical target of the antitumor indoleamine 2,3-dioxygenase inhibitory compound D-1-methyl-tryptophan. *Cancer Res.* **2007**, *67*, 7082-7.
- (80) Skehan, P.; Storeng, R.; Scudiero, D.; Monks, A.; McMahon, J.; Vistica, D.; Warren, J. T.; Bokesch, H.; Kenney, S.; Boyd, M. R. New colorimetric cytotoxicity assay for anticancer-drug screening. *J. Natl. Cancer Inst.* **1990**, *82*, 1107-12.
- (81) Baban, B.; Chandler, P.; McCool, D.; Marshall, B.; Munn, D. H.; Mellor, A. L. Indoleamine 2,3-dioxygenase expression is restricted to fetal trophoblast giant cells during murine gestation and is maternal genome specific. *J. Reprod. Immunol.* **2004**, *61*, 67-77.
- (82) Halgren, T. A. MMFF VI. MMFF94s option for energy minimization studies. *J. Comput. Chem.* **1999**, *20*, 720-729.
- (83) Halgren, T. A. MMFF VII. Characterization of MMFF94, MMFF94s, and other widely available force fields for conformational energies and for intermolecular-interaction energies and geometries. *J. Comput. Chem.* **1999**, *20*, 740-774.
- (84) Word, J. M.; Lovell, S. C.; Richardson, J. S.; Richardson, D. C. Asparagine and glutamine: Using hydrogen atom contacts in the choice of side-chain amide orientation. *J. Mol. Biol.* **1999**, *285*, 1735-1747.
- (85) Lovell, S. C.; Davis, I. W.; Arendall, W. B., III; de Bakker, P. I. W.; Word, J. M.; Prisant, M. G.; Richardson, J. S.; Richardson, D. C. Structure Validation by C α Geometry: ϕ , ψ and C β Deviation. *Proteins: Struct. Funct. Genet.* **2003**, *50*, 437-450.
- (86) Ponder, J. W.; Case, D. A. Force Fields for Protein Simulations. *Adv. Protein Chem.* **2003**, *66*, 27-85.
- (87) Thomsen, R.; Christensen, M. H. MolDock: A New Technique for High-Accuracy Molecular Docking. *J. Med. Chem.* **2006**, *49*, 3315-3321.
- (88) Jones, G.; Willet, P.; Glen, R. C.; Leach, A. R.; Taylor, R. Development And Validation Of A Genetic Algorithm For Flexible Docking. *J. Mol. Biol.* **1997**, *267*, 727-748.
- (89) Verdonk, M. L.; Cole, J. C.; Hartshorn, M. J.; W, M. C.; R.D., T. Improved Protein-Ligand Docking Using GOLD. *Proteins* **2003**, *52*, 609-623.
- (90) Morris, G. M.; Goodsell, D. S.; Halliday, R. S.; Huey, R.; Hart, W. E.; Belew, R. K.; Olson, A. J. Automated Docking Using a Lamarckian Genetic Algorithm and Empirical Binding Free Energy Function. *J. Comput. Chem.* **1998**, *19*, 1639-1662.

JM7014155